

Learning to Aggregate on Structured Data

Clemens Damke

March 20, 2020



PADERBORN UNIVERSITY
The University for the Information Society

Department of Electrical Engineering,
Computer Science and Mathematics
Warburger Straße 100
33098 Paderborn



Intelligent Systems and
Machine Learning Group (ISG)

Master Thesis

Learning to Aggregate on Structured Data

Clemens Damke

1. Reviewer Prof. Dr. Eyke Hüllermeier
Intelligent Systems and Machine Learning Group (ISG)
Paderborn University

2. Reviewer Prof. Dr. Axel-Cyrille Ngonga Ngomo
Data Science Group (DICE)
Paderborn University

March 20, 2020

Clemens Damke

Learning to Aggregate on Structured Data

Master Thesis, March 20, 2020

Reviewers: Prof. Dr. Eyke Hüllermeier and Prof. Dr. Axel-Cyrille Ngonga Ngomo

Supervisor: Vitalik Melnikov

Paderborn University

Intelligent Systems and Machine Learning Group (ISG)

Heinz Nixdorf Institute

Department of Electrical Engineering, Computer Science and Mathematics

Warburger Straße 100

33098 Paderborn

Abstract

Contents

| | | |
|----------|--|-----------|
| 1 | Introduction | 1 |
| 1.1 | Motivation | 1 |
| 1.2 | Goals | 2 |
| 1.3 | Structure | 2 |
| 2 | Related Work | 3 |
| 2.1 | Learning to Aggregate | 3 |
| 2.1.1 | Uninorm-Aggregation | 4 |
| 2.1.2 | OWA-Aggregation | 5 |
| 2.2 | Graph Characterization | 6 |
| 2.2.1 | The Graph Isomorphism Problem | 6 |
| 2.2.2 | Weisfeiler-Lehman Graph Colorings | 7 |
| 2.2.3 | Spectral Graph Theory | 13 |
| 2.3 | Graph Classification and Regression | 16 |
| 2.3.1 | Explicit Graph Embeddings | 16 |
| 2.3.2 | Graph Kernels | 18 |
| 2.3.3 | Graph Neural Networks | 20 |
| 3 | Learning to Aggregate on Graphs | 27 |
| 3.1 | A Generalized Definition of LTA | 27 |
| 3.2 | LTA Formulations of Existing GC/GR Methods | 30 |
| 3.2.1 | SVMs on Graph Embeddings as LTA Models | 30 |
| 3.2.2 | GCNNs as LTA Models | 35 |
| 3.3 | A Novel LTA-Inspired GCNN Architecture | 36 |
| 4 | Evaluation | 37 |
| 5 | Conclusion | 39 |
| 5.1 | Review | 39 |
| 5.2 | Future Directions | 39 |
| A | Appendix | 43 |
| | Bibliography | 45 |

Introduction

1.1 Motivation

The field of *machine learning* (ML) on graph-structured data has applications in many domains due to the general expressive power of graphs. The three most common types of graph ML problems are

1. **Link prediction:** A graph with an incomplete edge set is given and the missing edges have to be predicted. The suggestion of potential friends in a social network is a typical example for this.
2. **Vertex classification & regression:** Here a class or a score has to be predicted for each vertex of a graph. In social graphs this corresponds to the prediction of properties of individuals, e.g. personal preferences or gender. Another example is the prediction of the amount of traffic at the intersections of a street network.
3. **Graph classification & regression:** In this final problem type a single global class or continuous value has to be predicted for an input graph. The canonical example for this is the prediction of properties of molecule graphs, e.g. the toxicity or solubility of a chemical.

In this thesis we will focus on the last problem type, *graph classification and regression* (GC/GR). An ML method for this problem has to accept graphs of varying size and should be permutation invariant wrt. the order in which graph vertices are provided. Those requirements are not met by the commonly used learners that only accept fixed-size feature vectors as their input, e.g. *logistic regression models* (LRMs), *support vector machines* (SVMs) or *multilayer perceptrons* (MLPs).

A GC/GR method has to account for two central aspects of the problem: 1. Local structural analysis and 2. global aggregation. The first aspect is about the extraction of relevant features of substructures of the input graph. The latter is about the way in which the local features are combined into a final class or regression value. The existing GC/GR methods are mostly motivated by local structural graph analysis. The aspect of global aggregation on the other hand is less emphasized by those methods.

There is however a separate branch of research that specifically looks at the problem of learning aggregation functions, called *learning to aggregate* (LTA). Current LTA

approaches explicitly learn an aggregation functions for sets which can be interpreted as graphs without edges. The motivation for this thesis is to generalize LTA from sets to arbitrary graphs. The overall goal is to combine the aggregation learning perspective with existing GC/GR methods.

1.2 Goals

To extend LTA to graphs, three goals have to be achieved:

1. **Formalization of LTA:** Before LTA can be extended, its essential characteristics have to be defined. Those characteristics should provide the terminology to formally capture the differences and similarities between LTA and existing GC/GR methods.
2. **Give an LTA interpretation of GC/GR methods:** Using the LTA formalization, representative GC/GR approaches should be restated as LTA instances. Currently there is no comprehensive formulation of the relation between both fields of research; this is addressed by the the second goal.
3. **Define an LTA method for graphs:** Using the LTA perspective on GC/GR, hidden assumptions of the existing approaches should become clear and in which way they share the assumptions of LTA. The last goal is to use those insights to formulate an LTA-GC/GR method that combines ideas from the existing approaches with the LTA assumptions.

1.3 Structure

Chapter 2: Related Work

Chapter 3: Learning to Aggregate on Graphs

Chapter 4: Evaluation

Chapter 5: Conclusion

Related Work

Before combining LTA and GC/GR as described in section 1.2, we first give an overview of the state-of-the-art in both fields of research. This is done in three steps:

1. We begin with an overview of the existing LTA methods for unstructured inputs.
2. Then we look at the domain of structured inputs. To solve the GC/GR problem, relevant graphs characteristics have to be defined in order to determine the similarity and dissimilarity of graphs. We will look at three approaches for graph characterization: The graph isomorphism test, the so-called Weisfeiler-Lehman coloring and lastly the notion of graph spectra.
3. Based on the described graph characterization approaches, an overview of current GC/GR methods will then be given.

2.1 Learning to Aggregate

The class of LTA problems was first described by Melnikov and Hüllermeier [MH16]. There an input instance is understood as a composition $C = \{\{c_1, \dots, c_n\}\}$ of so-called constituents, i.e. as a variable-size multiset (denoted as $\{\cdot\}$). The assumption in LTA problems is that for all constituents $c_i \in C$ a local score $y_i \in \mathcal{Y}$ is either given or computable. The set of those local scores should be indicative of the overall score $y \in \mathcal{Y}$ of the composition C . LTA problems typically require two subproblems to be solved:

1. **Aggregation:** A variadic aggregation function $\mathcal{A} : \mathcal{Y}^* \rightarrow \mathcal{Y}$ that estimates composite scores has to be learned, i.e. $y \approx \hat{y} = \mathcal{A}(y_1, \dots, y_n)$. Typically the aggregation function \mathcal{A} should be associative and commutative to fit with the multiset-structure of compositions.
2. **Disaggregation:** In case the constituent scores y_i are not given, they have to be derived from a constituent representation, e.g. a vector $x_i \in \mathcal{X}$. To learn this derivation function $f : \mathcal{X} \rightarrow \mathcal{Y}$, only the constituent vectors $\{x_i\}_{i=1}^n$ and the composite score y is given. Thus the constituent scores y_i need to be *disaggregated* from y in order to learn f .

Overall LTA can be understood as the joint problem of learning the aggregation function \mathcal{A} and the local score derivation function f . Two main approaches to



Figure 2.1. Overview of the structure of LTA for multiset compositions.

represent the aggregation function in LTA problems have been explored.

2.1.1 Uninorm-Aggregation

The first approach uses *uninorms* [MH16] to do so. There the basic idea is to express composite scores as fuzzy truth assignments $y \in [0, 1]$. Such a composite assignment y is modeled as the result of a parameterized logical expression of constituent assignments $y_i \in [0, 1]$. As the logical expression that thus effectively aggregates the constituents, a uninorm U_λ is used. Depending on the parameter $\lambda \in [0, 1]$, U_λ combines a t-norm T and a t-conorm S which are continuous generalizations of logical conjunction and disjunction respectively. One popular choice of norms are the so-called Łukasiewicz norms:

$$\begin{aligned} \text{t-norm } T(a, b) &:= \max\{0, a + b - 1\}, & \text{t-conorm } S(a, b) &:= \min\{a + b, 1\}, \\ \text{uninorm } U_\lambda(a, b) &:= \begin{cases} \lambda T\left(\frac{a}{\lambda}, \frac{b}{\lambda}\right) & \text{if } a, b \in [0, \lambda] \\ \lambda + (1 - \lambda)S\left(\frac{a-\lambda}{1-\lambda}, \frac{b-\lambda}{1-\lambda}\right) & \text{if } a, b \in [\lambda, 1] \\ \lambda \min\{a, b\} & \text{else} \end{cases} \end{aligned} \quad (2.1)$$

At the extreme points $(0, 0)$, $(0, 1)$, $(1, 0)$ and $(1, 1)$, T and S coincide with the Boolean operators \wedge and \vee ; the values at all other points are interpolated as shown in fig. 2.2. The uninorm U_λ uses the conjunctive t-norm T for values below the threshold λ and the disjunctive t-conorm S for values above the threshold. U_λ therefore smoothly interpolates between a conjunctive and disjunctive operator with the extreme points $U_1 = T$ and $U_0 = S$.

Since t-norms and t-conorms are commutative and associative they can also be applied to non-empty sets of arbitrary size, i.e. $T(\{y_1, \dots, y_n\}) = T(y_1, T(\{y_2, \dots, y_n\}))$ with fixpoint $T(\{y\}) = y$. Using this extension, a uninorm U_λ can be applied to sets which turns it into a parameterized aggregation function $A_\lambda : [0, 1]^* \rightarrow [0, 1]$. In this simple model the LTA aggregation problem boils down to the optimization of λ . The LTA disaggregation problem is solved by jointly optimizing a logistic regression model, i.e. the constituent scores $\{y_i \in [0, 1]\}_{c_i \in C}$ are described by $y_i = (1 + \exp(-\theta^\top x_i))^{-1}$. Overall an LTA model is therefore described by the uninorm



Figure 2.2. The Łukasiewicz norms and the corresponding uninorm for $\lambda = 0.5$.

parameter λ and the regression coefficients θ .

2.1.2 OWA-Aggregation

Recently Melnikov and Hüllermeier [MH19] have looked at an alternative class of aggregation functions. Instead of using fuzzy logic to describe score aggregation, *ordered weighted average* (OWA) operators were used. OWA aggregators work by sorting the input scores and then weighting them based on their sort position, i.e.

$$\mathcal{A}_\lambda(y_1, \dots, y_n) := \sum_{i=1}^n \lambda_i y_{\pi(i)}, \quad (2.2)$$

where $\lambda \in \mathbb{R}^n$ is a weight vector with $\|\lambda\|_1 = 1$ and $\pi : [n] \rightarrow [n]$ is a sorting permutation of the input scores with $[n] := \{1, \dots, n\}$ and $y_i < y_j \Rightarrow \pi(i) < \pi(j)$. Depending on the choice of the vector λ , the OWA function \mathcal{A}_λ can express common aggregation functions like min (if $\lambda = (1, 0, \dots, 0)$), max (if $\lambda = (0, \dots, 0, 1)$) or the arithmetic mean (if $\lambda = (\frac{1}{n}, \dots, \frac{1}{n})$).

To deal with varying composition sizes n , the weights $\lambda_1, \dots, \lambda_n$ can however not be statically assigned. Instead they are interpolated using a so-called *basic unit interval monotone* (BUM) function $q : [0, 1] \rightarrow [0, 1]$. It takes constituent positions that are normalized to the unit interval, i.e. $\frac{i}{n} \in [0, 1]$. The BUM function q is then used to interpolate a weight for any normalized sort position via $\lambda_i := q\left(\frac{i}{n}\right) - q\left(\frac{i-1}{n}\right)$. Because q is monotone with $q(0) = 0$ and $q(1) = 1$, it always holds that $\|\lambda\|_1 = q(1) - q(0) = 1$. Using this model, the aggregation problem boils down to optimizing the shape of q .

In the OWA approach the BUM function q is modeled as a piecewise linear spline. This spline is described by $m + 1$ points $\left\{\left(\frac{j}{m}, a_j\right)\right\}_{j=0}^m$, the so-called knots of the spline. The curve of q is obtained by linearly interpolating between neighboring knots as shown in fig. 2.3. If $0 = a_0 \leq a_1 \leq \dots \leq a_m = 1$, q is a BUM function. The LTA aggregation problem is therefore solved by optimizing $a \in \mathbb{R}^{m+1}$ under this constraint. The disaggregation problem is tackled by adding the scores $y_1, \dots, y_M \in \mathbb{R}$ to the learnable parameters of the model where M is assumed to be the finite number of



Figure 2.3. Illustration of how a describes q and its relation to λ ($n = 4, m = 7$).

constituents. Currently the OWA approach requires all possible constituents to be part of the training dataset since it does not consider constituent features $x_i \in \mathcal{X}$ to predict the scores of previously unseen constituents.

2.2 Graph Characterization

Definition 2.1. A graph $G := (\mathcal{V}_G, \mathcal{E}_G)$ consists of a finite set of vertices $v_i \in \mathcal{V}_G$ and a set of edges $e_{ij} = (v_i, v_j) \in \mathcal{E}_G \subseteq \mathcal{V}_G^2$. Optionally discrete vertex labels $l_G[v_i] \in L_V$ or edge labels $l_G[e_{ij}] \in L_E$ may be associated with all vertices $v_i \in \mathcal{V}_G$ and edges $e_{ij} \in \mathcal{E}_G$ respectively. Also continuous feature vectors $x_G[v_i] \in \mathcal{X}_V, x_G[e_{ij}] \in \mathcal{X}_E$ may be given. If $\mathcal{X}_E = \mathbb{R}$, $x_G[e_{ij}]$ can be interpreted as an edge weight of e_{ij} .

In this thesis all graphs G are assumed to be undirected if not explicitly stated otherwise, i.e. $e_{ij} \in \mathcal{E}_G \leftrightarrow e_{ji} \in \mathcal{E}_G \wedge l_G[e_{ij}] = l_G[e_{ji}] \wedge x_G[e_{ij}] = x_G[e_{ji}]$. We denote the set of all undirected graphs as \mathcal{G} . Additionally we denote $G[S] := (S, \mathcal{E}_G \cap S^2)$ as the subgraph of G induced by $S \subseteq \mathcal{V}_G$.

To classify or score a graph, it first needs to be characterized by a set of relevant properties. The most strict characterization of a graph is its so-called *isomorphism class*. It uniquely identifies a graph but lacks any notion of similarity between non-identical graphs. We will begin with a brief definition of this strict isomorphism-based graph characterization. Then two less strict characterization approaches are described; the so called Weisfeiler-Lehman coloring and the notion of graph spectra. They are the theoretical foundation of many current GC/GR methods.

2.2.1 The Graph Isomorphism Problem

In order to process a graph G of size $n = |\mathcal{V}_G|$, one is forced to choose some encoding, e.g. an adjacency matrix $A_G \in \{0, 1\}^{n \times n}$. Such an encoding introduces a vertex ordering v_1, \dots, v_n that does not carry any semantic meaning. Consequently there are $n!$ equivalent encodings of G . To represent those encodings we introduce the

notion of ordered induced subgraphs.

Definition 2.2. For all vertex k -tuples $v = (v_1, \dots, v_k) \in \mathcal{V}_G^k$ let $\hat{v} = \text{set}(v) := \{v_i \mid i \in [k]\}$. Then $G[v] := (\hat{v}, \mathcal{E}_G \cap \hat{v}^2, v)$ is called the *ordered subgraph* of G induced by v . We denote the set of all ordered subgraphs with \mathcal{G}_{ord} . If $\hat{v} = \mathcal{V}_G$ and $k = |\mathcal{V}_G|$, we call v an *ordering* of G and $G[v]$ an *encoding* of G .

Definition 2.3. Two ordered induced subgraphs $G[v]$ and $H[w]$ with $(v_1, \dots, v_k) \in \mathcal{V}_G^k$ and $(w_1, \dots, w_k) \in \mathcal{V}_H^k$ are *equivalent* ($G[v] \equiv H[w]$) iff.

$$\begin{aligned} & \forall i, j \in [k] : (v_i, v_j) \in \mathcal{E}_G \leftrightarrow (w_i, w_j) \in \mathcal{E}_H \\ & \wedge \forall i, j \in [k] : l_G[v_i, v_j] = l_H[w_i, w_j] \quad \wedge \quad \forall i \in [k] : l_G[v_i] = l_H[w_i] \\ & \wedge \forall i, j \in [k] : x_G[v_i, v_j] = x_H[w_i, w_j] \quad \wedge \quad \forall i \in [k] : x_G[v_i] = x_H[w_i]. \end{aligned}$$

Using this notion of equivalence, we call $[G[v]] := \{G[w] \mid G[w] \equiv G[v] \wedge w \in \mathcal{V}_G^*\}$ the *ordered subgraph equivalence class* of $G[v]$.

Definition 2.4. Two graphs G and H are *isomorphic* ($G \simeq H$) iff. there are equivalent encodings $G[v] \equiv H[w]$ of them. Consequently $[G] := \{H \mid H \simeq G\}$ is called the *isomorphism class* of G .

The goal of the *graph isomorphism* (GI) problem is to check whether $G \simeq H$ for two arbitrary graphs. Even though there is no known universal polynomial algorithm that solves GI, Babai et al. [Bab+80] showed that almost all graphs can be trivially distinguished in linear time. More recently Babai [Bab15] also presented a quasipolynomial upper time bound for the remaining hard GI instances. For all practical purposes, GI can therefore be solved efficiently; e.g. via the nauty program [MP][MP13]. One important subroutine in most GI checkers is the Weisfeiler-Lehman algorithm which will be described next.

2.2.2 Weisfeiler-Lehman Graph Colorings

The *Weisfeiler-Lehman* (WL) algorithm [WL68][Cai+92] characterizes a graph G by assigning discrete labels $c \in \mathcal{C}$, called *colors*, to vertex k -tuples $(v_1, \dots, v_k) \in \mathcal{V}_G^k$, where $k \in \mathbb{N}_0$ is the freely choosable *WL-dimension*. A mapping $\chi_{G,k} : \mathcal{V}_G^k \rightarrow \mathcal{C}$ is called a *k-coloring* of G .

Definition 2.5. A coloring χ' *refines* χ ($\chi' \preceq \chi$) iff. $\forall a, b \in \mathcal{V}_G^k : \chi(a) \neq \chi(b) \rightarrow \chi'(a) \neq \chi'(b)$, i.e. χ' distinguishes at least those tuples that are distinguished by χ .

Definition 2.6. Two colorings χ and χ' are *equivalent* ($\chi \equiv \chi'$) iff. $\chi \preceq \chi' \wedge \chi' \succeq \chi$, i.e. χ is identical to χ' up to color substitutions.

The k -dimensional WL algorithm (k -WL) works by iteratively refining k -colorings

$\chi_{G,k}^{(0)} \succeq \chi_{G,k}^{(1)} \succeq \dots$ of a given graph G until the convergence criterion $\chi_{G,k}^{(i)} \equiv \chi_{G,k}^{(i+1)}$ is satisfied. We denote the final, maximally refined k -WL coloring with $\chi_{G,k}^*$.

Definition 2.7. The color distribution $dist_{\chi_{G,k}} : \mathcal{C} \rightarrow \mathbb{N}_0$ of a k -coloring $\chi_{G,k}$ counts each color $c \in \mathcal{C}$ in the coloring, i.e. $dist_{\chi_{G,k}}(c) := |\{v \in \mathcal{V}_G^k \mid \chi_{G,k}(v) = c\}|$.

Definition 2.8. Two graphs G and H are k -WL *distinguishable* ($G \not\simeq_k H$) iff. there exists a color $c \in \mathcal{C}$ s.t. $dist_{\chi_{G,k}^*}(c) \neq dist_{\chi_{H,k}^*}(c)$.

As we will see, the way in which WL colorings are refined is vertex order invariant; thus any difference in the final coloring of two graphs always implies the non-isomorphism of the colored graphs, i.e. $G \not\simeq_k H \implies G \not\simeq H$. The opposite does however not necessarily hold; two k -WL indistinguishable graphs are not always isomorphic, i.e. $\exists G, H : G \simeq_k H \wedge G \not\simeq H$.

In addition to the binary aspect of WL distinguishability and its relation to the GI problem, WL colorings are also useful for more fuzzy graph similarity comparisons as we will see in section 2.3.2 when we look at graph kernels. Before that however, the details of WL color refinement strategy have to be described. We begin with the color refinement algorithm for the most simple case of $k = 1$. Then the definitions and intuitions from the 1-dimensional case are extended to its higher-dimensional generalization. Lastly we will discuss the discriminative power of the WL algorithm and its relation to the WL-dimension k .

The 1-dimensional WL algorithm

In the 1-dimensional WL algorithm (1-WL), a color is assigned to each vertex of a graph. If the vertices $v \in \mathcal{V}_G$ of the input graph G are labeled, those labels $l_G[v] \in L_V \subseteq \mathcal{C}$ can be used as the initial graph coloring $\chi_{G,1}^{(0)}(v) := l_G[v]$. Since WL colors are inherently discrete, continuous vertex feature vectors $x_G[v]$ are not considered here. For unlabeled graphs a constant coloring is used, e.g. $\forall v \in \mathcal{V}_G : \chi_{G,1}^{(0)}(v) = \text{A}$ for some initial color $\text{A} \in \mathcal{C}$. In each iteration of the 1-WL color refinement algorithm, the following neighborhood aggregation scheme is used to compute a new color for all vertices:

Definition 2.9. $\chi_{G,1}^{(i+1)}(v) := h(\chi_{G,1}^{(i)}(v), \{\chi_{G,1}^{(i)}(u) \mid u \in \Gamma_G(v)\})$, with $\Gamma_G(v)$ denoting the set of adjacent vertices of $v \in \mathcal{V}_G$ and $h : \mathcal{C}^* \rightarrow \mathcal{C}$ denoting an injective hash function that assigns a unique color to each finite combination of colors.

In practice the hash function h is usually defined lazily by using $\mathcal{C} \subseteq \mathbb{N}$ and enumerating color combinations in whichever order they are hashed s.t. a new color is introduced every time a previously unseen color combination appears at runtime¹.

¹ Though \mathcal{C} is countably infinite, we assume it only contains the finite no. of colors in a dataset.



Figure 2.4. Example 1-WL color refinement steps. After two iterations the coloring stabilizes. Each vertex v is labeled with its current color and has its previous color and the colors of the hashed neighbors $\Gamma_G(v)$ written next to it (see definition 2.9).

The k -dimensional WL algorithm

As we just saw, the 1-WL algorithm iteratively refines colorings of single vertices. While the obtained colorings differ for most non-isomorphic graphs $G \not\simeq H$, 1-WL does not generally solve the GI problem as illustrated in fig. 2.5.



Figure 2.5. Two simple non-isomorphic graphs that are indistinguishable by 1-WL.

By extending WL to higher dimensions, such 1-WL indistinguishable cases can however be handled. Analogous to the 1-dimensional definition 2.9, the k -dimensional color refinement step is defined by

$$\begin{aligned} \text{Definition 2.10. } \chi_{G,k}^{(i+1)}(s) &:= h\left(\chi_{G,k}^{(i)}(s), \{\chi_{G,k}^{(i)}(s[u/1]), \dots, \chi_{G,k}^{(i)}(s[u/k])\} \mid u \in \mathcal{V}_G\right) \\ \text{with } s = (v_1, \dots, v_k) \in \mathcal{V}_G^k, \quad s[u/j] &:= (v_1, \dots, v_{j-1}, u, v_{j+1}, \dots, v_k). \end{aligned}$$

In 1-WL a vertex color is refined by combining the colors of neighboring vertices. In k -WL the color of a k -tuple $s \in \mathcal{V}_G^k$ is refined by combining the colors of its neighborhood which is defined as the set of all k -tuples in which at most one vertex differs from s . Note that each vertex k -tuple has one neighbor for each $u \in \mathcal{V}_G$, each of which is a k -tuple of vertex k -tuples. This more abstract notion of neighborhood is illustrated in fig. 2.6. For $k = 2$ this means that each potential edge $(v, w) \in \mathcal{V}_G^2$ has all possible paths of length 2 from v to w as its neighbors (see fig. 2.6b). Also note that, even though k -WL refines k -tuple colors, lower-dimensional structures still get their own colors since a tuple does not have to consist of distinct vertices, i.e. in k -WL the color of a single vertex $v \in \mathcal{V}_G$ is described by $\chi_{G,k}^*(s)$ for $s = (v, \dots, v) \in \mathcal{V}_G^k$.

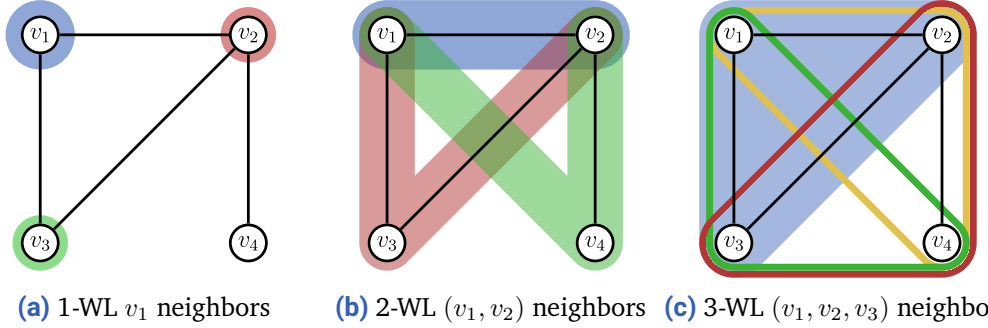


Figure 2.6. Tuple neighborhoods for different values of k . The vertices highlighted in blue form the root tuple $s \in \mathcal{V}_G^k$ whose neighbors are shown; for simplicity neighbors with $u \in s$ are left out (see definition 2.10). Each neighbor is highlighted with a different color, except for 3-WL where the red, green and yellow triples actually form the single neighbor for $u = v_4$.

Let us now look at how the tuple colors are initialized. For this we use the ordered subgraph equivalence classes $[G[s]]$ (see definition 2.3) which determine the initial color $\chi_{G,k}^{(0)}(v)$ of each k -tuple s . For $k = 1$ the equivalence class of a single vertex v directly corresponds to its label $l_G[v]$. More generally for $k > 1$ this means that

$$\chi_{G,k}^{(0)}(s) = \chi_{G,k}^{(0)}(t) \iff G[s] \equiv G[t]. \quad (2.3)$$

Note that there is a fundamental difference in how the adjacency information encoded in \mathcal{E}_G is used in 1-WL vs. k -WL: In 1-WL a vertex coloring by itself cannot encode adjacency which is why this information is explicitly incorporated in each refinement step via Γ_G (see definition 2.9). In k -WL on the other hand, each pair of vertices $(v, u) \in \mathcal{V}_G^2$ appears in at least one k -tuple (assuming $k \geq 2$) and therefore has at least one color which can implicitly encode the adjacency information. Edges and non-edges are colored differently in the initial coloring since $G[(v, u)] \neq G[(w, u)]$ if $(v, u) \in \mathcal{E}_G$ but $(w, u) \notin \mathcal{E}_G$; thus no explicit adjacency information is needed in the k -WL color refinement step in definition 2.10.

Discriminative Power of WL

Now we will look at the types of graphs that can be distinguished by WL in relation to the WL-dimension k . We begin by showing that the power of WL grows with k .

Lemma 2.11. $G \not\sim_k H \implies G \not\sim_{k+1} H$ ($(k+1)$ -WL is at least as powerful as k -WL).

Proof Sketch. All k -tuples can be mapped to $(k+1)$ -tuples via $\varphi(v_1, \dots, v_k) := (v_1, \dots, v_k, v_k)$. For each neighbor $(s[u/1], \dots, s[u/k])$ of $s \in \mathcal{V}_G^k$, there is a corresponding neighbor $(\varphi(s[u/1]), \dots, \varphi(s[u/k]), \varphi(s[u/k]))$ of $\varphi(s)$. Using eq. (2.3) (for $i = 0$) and definition 2.10 (for $i > 0$) it follows that $\forall s, t \in \mathcal{V}_G^k : \chi_{G,k}^{(i)}(s) \neq \chi_{G,k}^{(i)}(t) \rightarrow \chi_{G,k+1}^{(i)}(\varphi(s)) \neq \chi_{G,k+1}^{(i)}(\varphi(t))$. The lemma then follows by definition 2.8. \square

Proposition 2.12 (see Immerman and Lander [IL90] for the proof). *For all $k \in \mathbb{N}$ there are non-isomorphic graphs $G \not\simeq H$ of size $\mathcal{O}(k)$ with $G \simeq_k H$.*

Corollary 2.13. *The discriminative power of k -WL grows monotonously with k and never converges, i.e. for all $k \in \mathbb{N}$ there is an $l \in \mathbb{N}$ s.t. the set of k -WL distinguishable graphs is a proper subset of the $(k + l)$ -WL distinguishable graphs.*

Proof Sketch. Note that k -WL trivially solves the GI problem for all graphs of size $\leq k$ via the initial coloring (see eq. (2.3)). Using lemma 2.11 and proposition 2.12 the corollary directly follows. \square

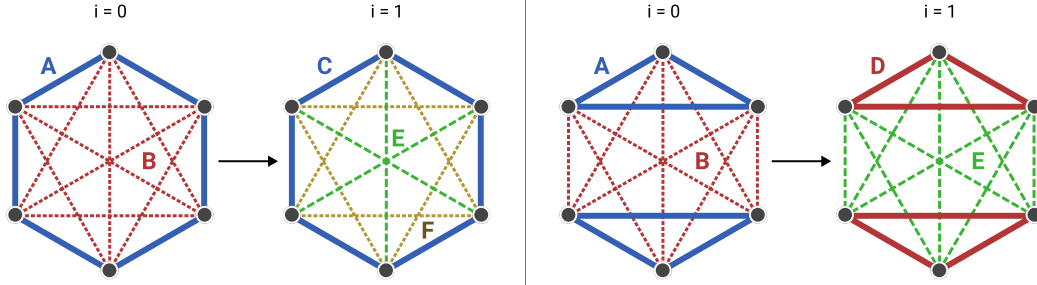


Figure 2.7. Two non-isomorphic graphs with $G \simeq_1 H$ and $G \not\simeq_2 H$.

Figure 2.7 illustrates corollary 2.13 by showing how 2-WL is able to distinguish the two 1-WL indistinguishable graphs from fig. 2.5. Since the time complexity of k -WL grows exponentially with k [IL90, cor. 1.9.7], it does not provide an efficient universal solution to GI. However it turns out that almost all graphs are WL distinguishable even for a small constant k .

For $k = 1$ Babai et al. [Bab+80] have shown that two randomly selected non-isomorphic graphs $G \not\simeq H$ of size n are 1-WL indistinguishable with probability $n^{-1/7}$. Thus 1-WL is already able to distinguish most graphs; it fails however to distinguish any pair of unlabeled d -regular graphs of the same size [IL90, cor. 1.8.5].

Definition 2.14. A graph G is called d -regular ($rg_d(G)$) iff. $\forall v \in \mathcal{V}_G : |\Gamma_G(v)| = d$.

We have already seen this in fig. 2.5 since the “six-cycle” and the “two-triangles” graphs are in fact both 2-regular and of size 6. This restriction alone is typically not an issue in the context of GC/GR though, as molecular structures or social interaction graphs for example are rarely perfectly regular. A more relevant restriction of 1-WL is the fact that it is unable to detect cycles of length $m \geq 3$.

Definition 2.15. k -WL computes a function $f : \mathcal{G} \rightarrow Y$ iff. that function can be expressed as $f(G) = g(\text{dist}_{\chi_{G,k}}^*)$ via some function $g : (\mathcal{C} \rightarrow \mathbb{N}) \rightarrow Y$.

Definition 2.16. k -WL counts a certain ordered subgraph $S \in \mathcal{G}_{ord}$ iff. it computes $\text{counts}_S(G) := |\{\text{set}(v) \mid v \in \mathcal{V}_G^* \wedge G[v] \equiv S\}|$ (see definition 2.2). Similarly k -WL detects an ordered subgraph S iff. it computes $\text{contain}_S(G) := \mathbb{1}[\text{counts}_S(G) > 0]$, with $\mathbb{1}$ denoting the indicator function.

To see why 1-WL is unable to detect m -cycles in graphs, note that fig. 2.5 already contradicts the positive statement for $m = 3$; this counterexample can be trivially generalized to all larger m by replacing the “six-cycle” graph with a “ $(2m)$ -cycle-graph” graph and the “two-triangles” graph with a “two- m -cycles” graph which preserves the 2-regularity and therefore the 1-WL indistinguishability.

This cycle-detection restriction of 1-WL is relevant in practice because cycle counts are used in many domains to analyze graphs, e.g. triangle counts are commonly used in social network analysis to find interaction clusters [Mil02][New03][Wel+07] and the detection of 4-, 5- or 6-cycles is required to determine important chemical properties like the aromaticity of a molecule [AB73][Kek66].

If we increase the WL-dimension to $k = 2$, the described 1-WL restrictions no longer apply. 2-WL is able to distinguish more than $1 - \mathcal{O}(1/n)$ of the regular n -vertex graphs [IL90, cor. 1.8.6] and can even count cycles:

Proposition 2.17 (see Fürer [Fü17] and Arvind et al. [Arv+19] for the full proof). *2-WL is able to count m -cycles for $m \leq 7$ but it cannot detect 8-cycles.*

Proof Sketch. Only the idea behind triangle and 4-cycle counting is outlined here to give an intuition for why proposition 2.17 holds. Note that the 2-WL neighbors of each edge $(v, w) \in \mathcal{E}_G$ correspond to all possible paths (v, u, w) of length 2, i.e. all possible triangles. By definition 2.10 there must thus be a color subset $C_j^\triangle \subseteq \mathcal{C}$ representing that an edge is involved in exactly j triangles after one refinement step. 2-WL then trivially counts triangles by setting $g(\text{dist}_\chi) = \frac{1}{3} \sum_j j \sum_{c \in C_j^\triangle} \text{dist}_\chi(c)$ to satisfy definition 2.15. Analogously for 4-cycles, let $C_j^\square \subseteq \mathcal{C}$ be the colors indicating a non-edge $(v, w) \notin \mathcal{E}_G$ with j common vertex neighbors $u \in \Gamma_G(v) \cap \Gamma_G(w)$. The number of 4-cycles is then determined by the colors of the diagonals through them via $g(\text{dist}_\chi) = \frac{1}{2} \sum_{j \geq 2} \binom{j}{2} \sum_{c \in C_j^\square} \text{dist}_\chi(c)$. Using a similar but more involved combinatorial argument requiring multiple color refinement steps, 5-, 6- & 7-cycle counting can be shown. \square

As we just saw, 2-WL is significantly more powerful than 1-WL. Though, by proposition 2.12, there are of course still 2-WL indistinguishable graphs; among others those are the strongly regular graphs $srg_{n,d,\lambda,\mu}(G)$.

$$\begin{aligned} \text{Definition 2.18. } srg_{n,d,\lambda,\mu}(G) \iff & |\mathcal{V}_G| = n \quad \wedge \quad \forall v \in \mathcal{V}_G : |\Gamma_G(v)| = d \\ & \wedge \forall (v, w) \in \mathcal{E}_G : |\Gamma_G(v) \cap \Gamma_G(w)| = \lambda \\ & \wedge \forall (v, w) \in \mathcal{V}_G^2 \setminus \mathcal{E}_G : |\Gamma_G(v) \cap \Gamma_G(w)| = \mu \end{aligned}$$

Generally this restriction of 2-WL is not an issue since strongly regular graphs do not appear in typical GC/GR datasets. By going to $k = 3$, even some strongly regular graphs as well as all planar graphs can be distinguished though [Kie+17]. Apart from that there are currently few results regarding the classes of distinguishable graphs and computable functions for even higher WL-dimensions.

2.2.3 Spectral Graph Theory

Let us now look at an alternative perspective on graph characterization which is provided by *spectral graph theory*. While WL characterizes a graph via its color distribution $\text{dist}_{\chi_{G,k}^*}$, the spectral approach uses its so-called *spectrum* $\lambda_G = (\lambda_{G,1}, \dots, \lambda_{G,n}) \in \mathbb{R}^n$ where $n = |\mathcal{V}_G|$. The key idea behind this is to interpret the adjacency matrix $A_G \in \mathbb{R}^{n \times n}$ of G not simply as an encoding of the edges ($A_{G,i,j} = \mathbb{1}[(v_i, v_j) \in \mathcal{E}_G]$) but as a linear operator $A_G : (\mathcal{V}_G \rightarrow \mathbb{R}) \rightarrow (\mathcal{V}_G \rightarrow \mathbb{R})$ acting on the vector space of real-valued functions with a vertex domain. This means that A_G transforms so-called *graph signals* $x : \mathcal{V}_G \rightarrow \mathbb{R}$ which are functions assigning *signal strengths* to vertices. By applying $A_G x$ the signal strength $x[v_i]$ of each vertex is added to the signal strengths of its neighbors $\Gamma_G(v_i)$. Using this functional perspective, one can characterize graphs via the *Fourier transform* (FT). We will now see how this is done; however, since a comprehensive description of spectral graph theory would exceed the scope of this thesis, only a brief overview will be given. For a more detailed introduction to the field we refer to Shuman et al. [Shu+13].

The classical Fourier transform Let us begin by describing the FT for the more common case of functions with real domains. All functions $f : \mathbb{R} \rightarrow \mathbb{R}$ can be interpreted as infinite-dimensional vectors $f = \int_{\mathbb{R}} f(t) b_t dt$ with $b_t : \mathbb{R} \rightarrow \mathbb{R}$ being a standard basis vector/function defined as $b_t(s) := \begin{cases} 1 & \text{if } s = t \\ 0 & \text{else} \end{cases}$. The values of f are then described as its b_t components $\langle b_t, f \rangle = f(t)$, where $\langle b_t, \cdot \rangle = \delta_t(\cdot)$ denotes the Dirac delta function translated by t . The Fourier transform $\hat{f} = \mathcal{F}(f)$ of f corresponds to a change of basis from the standard basis vectors b_t to the Fourier basis vectors $u_{\xi}(t) := e^{2\pi i \xi t}$, i.e. $f = \int_{\mathbb{R}} \hat{f}(t) u_{\xi} dt$. The Fourier basis is characterized by the fact that it is an eigenbasis of the so-called *Laplace operator* Δ , i.e. $\Delta u_{\xi} = \lambda_{\xi} u_{\xi}$ with λ_{ξ} being the eigenvalue corresponding to u_{ξ} . In the real domain this Laplace operator Δ is effectively the same as the second-derivative $\frac{d^2}{dt^2}$. Thus it is easy to see that indeed $\Delta u_{\xi} = -\frac{d^2}{dt^2} u_{\xi} = \lambda_{\xi} u_{\xi}$ for $\lambda_{\xi} = (2\pi\xi)^2$.

The graph Fourier transform To extend the notion of the FT from real functions $f : \mathbb{R} \rightarrow \mathbb{R}$ to graph signals $x : \mathcal{V}_G \rightarrow \mathbb{R}$ we need to define a graph variant of the Laplace operator Δ . It turns out that there are multiple possible ways to do so, the most simple being the so-called *combinatorial graph Laplacian*.

Definition 2.19. The combinatorial graph Laplacian $L_G \in \mathbb{R}^{n \times n}$ is defined as

$$L_G := D_G - A_G \quad \text{with the degree matrix } D_G := \begin{pmatrix} d_1 & & \\ & \ddots & \\ & & d_n \end{pmatrix}, d_i := |\Gamma_G(v_i)|.$$

Using this definition, applying $L_G x$ is analogous to taking the second derivative $\frac{d^2}{dt^2} f$.

Putting both Laplacian variants, L_G and $\frac{d^2}{dt^2}$, side-by-side gives an intuition for why this is the case:

$$-\frac{d^2}{dt^2} f(t) = \lim_{h \rightarrow 0} \frac{1}{h^2} (\underbrace{f(t) - f(t-h)}_{\Delta_{t,t-h}} + \underbrace{f(t) - f(t+h)}_{\Delta_{t,t+h}}) \quad \left| \quad L_G x[v] = \sum_{u \in \Gamma_G(v)} \underbrace{(x[v] - x[u])}_{\Delta_{v,u}} \right.$$

The second derivative of a function f essentially averages the value differences in the neighborhood of a point t . For real-valued functions this neighborhood only consists of the two infinitesimally close points to the left and to the right of t , i.e. $t-h$ and $t+h$. The combinatorial graph Laplacian represents the same operation, where each point/vertex v might however have more than two neighbors $u \in \Gamma_G(v)$ that need to be averaged.

The FT of a graph signal x then is $\hat{x}[i] = \langle u_{G,i}, x \rangle$ with $u_G = \{u_{G,i}\}_{i=1}^n$ being the eigenvectors of L_G , s.t. $x = \sum_{i=1}^n \hat{x}[i] u_{G,i}$. Since the set of Laplacian eigenvectors is finite, we can express the graph FT \mathcal{F}_G as a change of basis matrix

$$U_G = \begin{pmatrix} u_{G,1,1} & \cdots & u_{G,1,n} \\ \vdots & \ddots & \vdots \\ u_{G,n,1} & \cdots & u_{G,n,n} \end{pmatrix} \in \mathbb{R}^{n \times n}. \text{ Similarly the inverse FT can be expressed}$$

as $\mathcal{F}^{-1} = U_G^{-1} = U_G^\top$ because U_G is a real orthogonal matrix. To see why this is the case, note that L_G is guaranteed to only have real eigenvectors u_G and eigenvalues λ_G due to the fact that we only consider undirected graphs with symmetric adjacency matrices A_G .

Interpretation of the spectrum By convention we assume that the eigenvalues are ordered ascendingly: $\lambda_{G,0} \leq \dots \leq \lambda_{G,n}$. Those eigenvalues are called the *spectrum of G* and they are a vertex-permutation-invariant graph characterization. Intuitively those eigenvalues describe the connectivity between different parts of the graph. The first eigenvalues represent connectivity at a general, coarse level while the last eigenvalues represent the connectivity of finer substructures. Figure 2.8 illustrates this idea. A concrete example for the relation between a graph's structure and its spectrum is the fact that a graph with m connected components has exactly m zero eigenvalues, i.e. $0 = \lambda_{G,1} = \dots = \lambda_{G,m} < \lambda_{G,m+1}$. For a more detailed discussion of this relation we refer to Das [Das04]. We will now instead look at the discriminative power of the spectrum.

Definition 2.20. Two graphs G and H are *cospectral* ($G \simeq_\lambda H$) iff. $\forall i : \lambda_{G,i} = \lambda_{H,i}$.

Spectral graph comparisons Alzaga et al. [Alz+10] have shown that, while the cospectrality test can be more powerful than 1-WL, it is always weaker than 2-WL, i.e. $G \simeq_2 H \implies G \simeq_\lambda H$. Despite this limit on the discriminative power of the graph spectrum, it is still useful for determining graph similarity, e.g. by defining a distance measure on the vector space of spectra (see Gu et al. [Gu+15]).

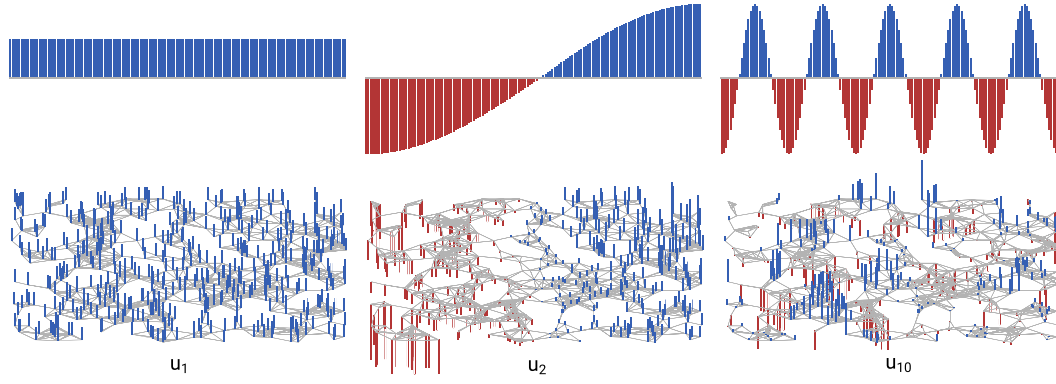


Figure 2.8. Comparison between the basis functions/vectors of the real domain FT and the graph FT. For the eigenfunctions on the upper half only the real cosine components of the complex exponentials are shown.

BASED ON: [SHU+13]

As briefly mentioned before, the combinatorial graph Laplacian L_G is not the only possible choice of graph Laplacian. Note that the eigenvalues of L_G grow with the number of edges². Consequently a small graph G will typically have a large spectral distance to a large graph H (assuming $|\mathcal{V}_G| \ll |\mathcal{V}_H|$) irrespective of their similarity when ignoring the scale difference. In domains where the absolute size of a graph should not influence its spectral characterization, it can therefore be useful to normalize the spectrum. One common way to do so is via the so-called *symmetric normalized Laplacian* L_G^{sym} .

Definition 2.21. $L_G^{\text{sym}} := D^{-\frac{1}{2}} L_G D^{-\frac{1}{2}}$ is the symmetric normalized Laplacian of G .

The eigenvalues $\lambda_{G,i}^{\text{sym}}$ of this Laplacian all lie in the range $[0, 2]$. Figure 2.9 illustrates how this makes it possible to compare the structure of graphs across varying vertex counts. Besides L_G^{sym} there are also other ways to normalize the spectrum, e.g. by using the random walk Laplacian $L_G^{\text{rw}} := D^{-1} L_G$, which will however not be covered here (see Shuman et al. [Shu+13]).

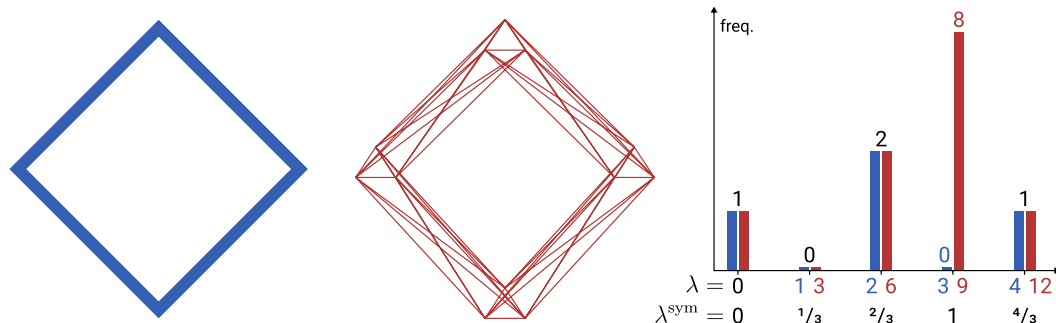


Figure 2.9. Comparison of the unnormalized L_G spectrum and the normalized L_G^{sym} spectrum. Two structurally similar graphs of different size are compared. The **large graph** is derived by replacing each vertex of the **small 4-cycle graph** by a triangle. While their unnormalized spectra have different absolute ranges ($[0, 4]$ vs. $[0, 12]$), the histogram on the right shows that their normalized eigenvalue distributions align.

² This is trivially shown by $\sum_{i=1}^n \lambda_{G,i} = \text{Tr}(L_G) = \text{Tr}(D_G) = |\mathcal{E}_G|$.

2.3 Graph Classification and Regression

Now that we have looked at the WL- and spectrum-based graph characterization approaches, we will see how those can be used to learn models that solve the *graph classification and regression* (GC/GR) problem. The existing approaches to tackle the GC/GR problem can be categorized into three main families: 1. Explicit graph embeddings, 2. graph kernels and 3. graph neural networks. In the following sections the characteristics of those families are described and a brief overview of specific methods is given.

2.3.1 Explicit Graph Embeddings

The basic idea of explicit graph embedding approaches is to map a graph $G \in \mathcal{G}$ to some vector in a finite vector space $\mathcal{X} = \mathbb{R}^d$. A function $\varphi : \mathcal{G} \rightarrow \mathcal{X}$ is called a *graph embedding function*. By embedding a graph into \mathcal{X} , any classification or regression algorithm that works with vectors can then be applied to solve the GC/GR problem.

The so-called vertex embedding problem is closely related to the graph embedding problem. As the name suggests, a *vertex embedding function* φ_G maps all vertices $v \in \mathcal{V}_G$ to \mathcal{X} . The embedding vector $\varphi_G(v)$ ideally encodes relevant information about a vertex and its structural position in G . It can be used to solve the vertex classification and regression problem via arbitrary ML methods for vectors. We will now look at two main families of explicit graph and vertex embedding approaches.

Fingerprint Embeddings

The first works on graph embeddings were motivated by the study of chemical structures [AB73][WW86]. There a molecule can be interpreted as a labeled graph for which the GC/GR problem corresponds to the prediction of some chemical property, e.g. toxicity or solubility. So-called *fingerprint embeddings* try to match a fixed set of subgraphs S_1, \dots, S_d to the input graph. The embedding of a graph G is a binary vector $\varphi_{\text{FP}}(G) \in \{0, 1\}^d$ with $\varphi_{\text{FP}}(G)[i] := \text{contain}_{S_i}(G)$ (see definition 2.16). Alternatively a fingerprint embedding can additionally encode multiplicities via $\varphi_{\text{FP}}(G)[i] := \text{count}_{S_i}(G) \in \mathbb{N}_0$.

This simple approach usually requires a careful choice of subgraphs but can still be competitive with the other more recent approaches we will look at in the following sections. Fingerprint embeddings are for example used in multiple state-of-the-art toxicity prediction tools like RASAR [Lue+18][Tox], ProTox [Drw+14][Ban+18a][Ban+18b] or the Toxicity Estimation Software Tools [Tes].

Skip-gram inspired Embeddings

Skip-gram embeddings were introduced by Mikolov et al. as part of the well-known `word2vec` [Mik+13] word embedding method from natural language processing. While a fingerprint embedding explicitly assigns an interpretation to each embedding dimension (i.e. to each standard basis vector), a skip-gram embedding only optimizes the distance between embedding vectors based on the similarity of the embedded instances without providing an interpretation of the embedding dimensions.

word2vec Let us first look at the `word2vec` skip-gram method. It gets a sequence of words (w_0, \dots, w_n) as input and outputs embedding vectors $\varphi(w_0), \dots, \varphi(w_n) \in \mathbb{R}^d$. To do this the context $\Gamma_k(w_i) = \{w_{i-k}, \dots, w_{i+k}\}$ is computed for all words where w_i is the so-called *context root*. The word contexts are then used to optimize the following log-likelihood objective:

$$\max_{\varphi, \varphi_\Gamma} \sum_{i=1}^n \log P(\Gamma_k(w_i) | w_i) = \max_{\varphi, \varphi_\Gamma} \sum_{i=1}^n \sum_{w_j \in \Gamma_k(w_i)} [\varphi(w_i)^\top \varphi_\Gamma(w_j) - \log Z_{w_i}] \quad (2.4)$$

with $P(\Gamma_k(w_i) | w_i) := \overbrace{\prod_{w_j \in \Gamma_k(w_i)} \frac{\exp(\varphi(w_i)^\top \varphi_\Gamma(w_j))}{Z_{w_i}} }^{P(w_j | w_i)}$ and $Z_{w_i} := \sum_{j=1}^n \exp(\varphi(w_i)^\top \varphi_\Gamma(w_j))$

`word2vec` essentially uses an expectation maximization scheme to maximize the probabilities $P(w_j | w_i)$ of observing the context words $w_j \in \Gamma_k(w_i)$ of all words w_i . Those probabilities are described by the overlap of the embeddings $\varphi(w_i)$ of words w_i and the embeddings $\varphi_\Gamma(w_j)$ of their context words w_j . Intuitively this means that words with similar contexts will be mapped close to each other in the embedding space. Note that `word2vec` actually finds two embeddings $\varphi(w)$ and $\varphi_\Gamma(w)$ for each word of which only the first is returned. The two embeddings represent two different perspectives on words: φ describes a word w_i as the root of a context $\Gamma_k(w_i)$, φ_Γ on the other hand describes a word w_j as part of a context $\Gamma_k(w_i) \ni w_j$.

Vertex Embeddings Skip-gram embeddings can be naively extended to graphs by realizing that `word2vec` effectively already is a vertex embedding method for linear graphs in which $\Gamma_k(v)$ is simply the k -neighborhood of the vertex/word v . The problem with this naïve extension is that the sizes of k -neighborhoods in arbitrary graphs can be much larger and often tend to grow exponentially with k . To deal with this computational problem the so-called DeepWalk [Per+14] and node2vec [GL16] methods perform random walks of fixed length to effectively take samples from the neighborhood of vertices. Both methods only differ in the transition matrix that is used for the random walk. Another difference of DeepWalk and node2vec compared to `word2vec` is the so-called *feature space symmetry* which states that the context root interpretation (φ) of a vertex should be symmetric to its context element

interpretation (φ_Γ), i.e. $\varphi = \varphi_\Gamma$. The combination of random walk context sampling and the feature space symmetry assumption can be used to compute vertex embeddings even for very large graphs.

Graph Embeddings Skip-gram methods can not only be used for vertex embeddings but also to embed entire graphs. One way to do this is via the graph2vec [Nar+17] method. It is inspired by doc2vec [LM14] which in turn is based on word2vec. graph2vec gets a set of graphs $\mathcal{G}' = \{G_1, \dots, G_N\}$ as input and outputs graph embeddings $\varphi(G_1), \dots, \varphi(G_N)$. While in word2vec every word can be a context root as well as a context element, graph2vec uses the graphs \mathcal{G}' as context roots. The context $\Gamma_T(G_i)$ of a graph G_i is defined as

$$\Gamma_T(G_i) := \bigcup_{v_j \in \mathcal{V}_{G_i}} \left\{ \chi_{G_i, 1}^{(t)}(v_j) \right\}_{t=0}^T \quad \text{with } T \in \mathbb{N} \text{ and } \chi_{G_i, 1}^{(t)} \text{ as in definition 2.9.} \quad (2.5)$$

Intuitively this context can be understood as the set of 1-WL-distinguishable subgraphs of G_i with diameter $\leq 2T$. Since WL is used to identify distinct subgraphs, graph2vec can only be applied to graphs with discrete vertex labels. Using the previous definitions, the context root embedding function has the signature $\varphi : \mathcal{G} \rightarrow \mathbb{R}^d$ while the context element embedding function is of type $\varphi_\Gamma : \bigcup_{G_i \in \mathcal{G}} \Gamma_T(G_i) \rightarrow \mathbb{R}^d$. To find those embeddings the word2vec objective from eq. (2.4) is reused. Analogous to word2vec, graph2vec therefore embeds graphs that share subgraphs close to each other, whereas graphs that do not share substructures tend to be embedded further away from each other.

2.3.2 Graph Kernels

Instead of mapping a graph into an explicitly defined vector space of fixed dimension, one can also do so implicitly by employing the kernel trick. There is a large variety of so-called *graph kernels* (GKs) to do this. GKs can be used in combination with any kernelized learner, typically SVMs, to solve the GC/GR problem. While there is a large variety of different GKs [Kri+20], we will focus on those that are based on the previously described family of WL algorithms.

WL subtree kernel One well-known GK is based directly on the 1-WL coloring algorithm, the so-called *WL subtree kernel* [She+11]. It uses the mapping

$$\varphi_{ST}(G) := \bigoplus_{t=0}^T \left(dist_{\chi_{G, 1}^{(t)}}(c) \right)_{c \in \mathcal{C}} \quad \text{with } \oplus \text{ denoting vector concatenation.} \quad (2.6)$$

$\varphi_{ST}(G)$ encodes the color counts across a fixed number T of 1-WL refinement steps. Via this mapping, the WL subtree kernel function $k_{ST} : \mathcal{G} \times \mathcal{G} \rightarrow \mathbb{R}$ can then be simply written as the standard inner vector product $k_{ST}(G, H) := \langle \varphi_{ST}(G), \varphi_{ST}(H) \rangle$.

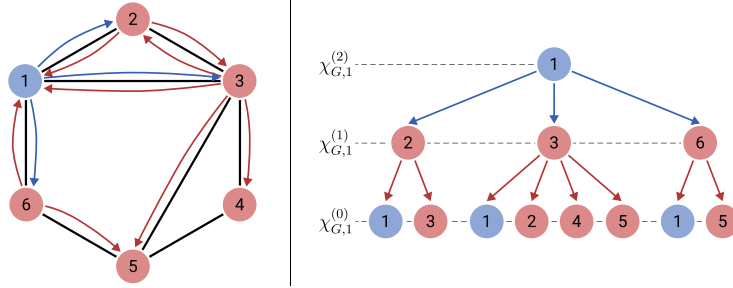


Figure 2.10. Illustration of the correspondence between the WL color $\chi_{G,1}^{(t)}(v)$ and the breadth-first subtree of depth t rooted at v (for $t = 2$ and $v = \textcircled{1}$). An arrow $A \rightarrow B$ indicates that the refined color of A depends on the color of B . BASED ON: [SHE+11]

Figure 2.10 illustrates how this definition relates to subtrees. Since all vertex colors $c \in \mathcal{C}$ correspond to a subtree isomorphism class, $k_{\text{ST}}(G, H)$ effectively computes the similarity of G and H by comparing their local subtree structures of depth at most T . Note that the underlying mapping φ_{ST} cannot be computed independently for each graph $G \in \mathcal{G}_D \subseteq \mathcal{G}$ in a given training dataset \mathcal{D} since the set of colors $c \in \mathcal{C}$ introduced by the hashing function h is conjointly determined by all graphs \mathcal{G}_D (see definition 2.9). Consequently the dimensionality d of $\varphi_{\text{ST}}(G) \in \mathbb{N}^d$ varies, depending on the entire dataset \mathcal{D} .

WL shortest path kernel Extending the idea of the WL subtree kernel, the *WL shortest path kernel* [She+11][BK05] adds global structural information to the local subtree comparisons. The i -th component of a graph's shortest path vector $\varphi_{\text{SP}}(G)$ corresponds to the 4-tuple $(t_i, a_i, b_i, d_i) \in \{0, \dots, T\} \times \mathcal{C} \times \mathcal{C} \times \mathbb{N}_0$ and its value is described by

$$\varphi_{\text{SP}}(G)[i] := \left| \left\{ (v, u) \in \mathcal{V}_G^2 \mid \chi_{G,1}^{(t_i)}(v) = a_i \wedge \chi_{G,1}^{(t_i)}(u) = b_i \wedge d_{\text{SP}}(v, u) = d_i \right\} \right|, \quad (2.7)$$

with $d_{\text{SP}}(v, u)$ denoting the length of the shortest path from v to u in G . Analogous to k_{ST} , the shortest path kernel function is defined as $k_{\text{SP}}(G, H) := \langle \varphi_{\text{SP}}(G), \varphi_{\text{SP}}(H) \rangle$. Since $\varphi_{\text{SP}}(G)$ has one component for each possible 4-tuple (t_i, a_i, b_i, d_i) , its dimensionality grows quadratically with the total number of introduced 1-WL colors \mathcal{C} and linearly with the length of the longest shortest path $\max_{G \in \mathcal{G}_D, (v,u) \in \mathcal{V}_G^2} d_{\text{SP}}(v, u)$. While this approach is computationally significantly more expensive than the subtree kernel, it also has a higher discriminative power and allows the shortest path kernel to distinguish even some 1-WL indistinguishable graphs. The subtree kernel only compares graphs by the presence of local subtrees; the shortest path kernel additionally checks how well the distances between those subtrees align. Looking back at the 1-WL indistinguishable “six-cycle”/“two-triangles” example from fig. 2.5, we see that this additional information distinguishes the two graphs due to the fact that the longest shortest path in a six-cycle has length 3 while the longest shortest path in a triangle is of length 1.

Higher dimensional WL kernels Instead of incorporating shortest path information to increase the power of the WL kernel, one can alternatively just increase the WL-dimension k . A naïve generalization of the 1-WL subtree kernel would simply use eq. (2.6) but with the k -WL colorings $\chi_{G,k}^{(t)}$ instead of $\chi_{G,1}^{(t)}$. The problem with this approach is that the runtime of WL increases exponentially with k ; even for $k = 2$ the cost often becomes infeasibly high when working with large graphs. To tackle this problem Morris et al. [Mor+17] proposed a combination of two optimizations:

1. **k -multisets:** The first optimization is to assign colors to vertex k -multisets instead of vertex k -tuples, where a k -multiset is any multiset $s \subseteq \mathcal{V}_G$ with $|s| = k$. This reduces the amount of colors that have to be refined in each WL iteration by a factor of $k!$. Based on definition 2.10, the multiset color refinement step is defined as

$$\chi_{G,k}^{(t+1)}(s) := h \left(\chi_{G,k}^{(t)}(s), \{ \{ \chi_{G,k}^{(t)}(s \setminus \{v\} \cup \{u\}) \mid v \in s \} \mid u \in \mathcal{V}_G \} \right). \quad (2.8)$$

Even though this simplification generally reduces the discriminative power of the kernel, for $k = 2$ specifically no information and therefore no power is lost by replacing the tuples (v, u) and (u, v) with $\{v, u\}$ since the undirectedness of graphs implies that $\chi_{G,2}^{(t)}(v, u) = \chi_{G,2}^{(t)}(u, v)$ even when doing tuple-based color refinement.

2. **Neighborhood localization:** The second optimization uses the fact that most real-world graphs tend to be sparse [Chu10], i.e. $|\mathcal{E}_G| = \mathcal{O}(|\mathcal{V}_G|)$. The multiset-based k -WL algorithm refines the color of a k -multiset s by hashing the colors of its neighbors as defined in eq. (2.8) where there is one neighbor per vertex $u \in \mathcal{V}_G$. By the sparsity assumption, most of those vertices u are however not connected with any of the vertices in s , i.e. $u \notin \Gamma_G(s)$ with $\Gamma_G(s) := \bigcup_{v \in s} \Gamma_G(v)$. The refinement runtime can therefore often be reduced significantly by only considering “local” neighbors $u \in \Gamma_G(s)$ instead of the “global” neighborhood $u \in \mathcal{V}_G$ in eq. (2.8).

We call the kernel that only uses the first optimization k -GWL (k -dim. global WL) and the kernel that uses both optimizations k -LWL (k -dim. local WL). Morris et al. [Mor+17] have empirically shown that focusing on local graph structures via LWL often actually performs better than the computationally more expensive GWL kernel.

2.3.3 Graph Neural Networks

The last family of GC/GR approaches we will look at is that of *graph neural networks* (GNNs). The idea to feed a graph into a *neural network* (NN) was first described by Gori et al. [Gor+05]. Since then many variants and extensions of that idea have been

proposed [Wu+19]. We will focus specifically on the so-called *graph convolutional neural networks* (GCNNs) which can be divided into two variants: Spectral and spatial GCNNs.

Spectral GCNNs

The class of spectral GCNNs is motivated by spectral graph theory (see section 2.2.3). A spectral GCNN expects a graph G with real vertex feature vectors $x_G[v_i] \in \mathbb{R}^d$ as its input. Those feature vectors are typically one-hot encodings of labels or, if no such information is provided, vertex embedding vectors (see section 2.3.1).

We call $X_G := \begin{pmatrix} x_G[v_1] \\ \vdots \\ x_G[v_n] \end{pmatrix} \in \mathbb{R}^{n \times d}$ the vertex feature matrix of G . Note that each

of the d columns of X_G can be interpreted as a separate graph signal function $x_{G,j} : \mathcal{V}_G \rightarrow \mathbb{R}$ for $j \in [d]$. The core idea of spectral GCNNs is to learn a graph convolution kernel g , similar to the grid kernels in conventional *convolutional neural networks* (CNNs) [LB98]. The problem with this idea is that the convolution operation $g * x$ requires some notion of distance in order to “move” the kernel g over the function x . Graphs do not generally satisfy this requirement, i.e. the notion of a vertex distance $\|v_i - v_j\|$ is not clearly defined. Via the convolution theorem $g * x = \mathcal{F}^{-1}(\hat{g} \odot \hat{x})$ we can however still define a graph convolution operator that works directly in the spectral domain:

$$g * x_{G,j} := U_G^\top (\hat{g} \odot (U_G x_{G,j})) \text{ with } \odot \text{ denoting element-wise multiplication. (2.9)}$$

To see the connection to the convolution theorem, remember that the Laplacian eigenvector matrices U_G and U_G^\top correspond to the FT \mathcal{F} and inverse FT \mathcal{F}^{-1} respectively. In this formulation of convolution the Fourier transformed kernel \hat{g} can be interpreted as a spectral filter, i.e. it dampens or amplifies certain eigenvector components of a graph. Bruna et al. [Bru+13][Hen+15] first described a GNN architecture that learns such a spectral filter \hat{g} . Since a GNN has to accept many different graphs of varying size n , the filter can however not be learned as a direct mapping $\hat{g} : [n] \rightarrow \mathbb{R}$. Therefore it is not expressed in terms of the indices i of specific eigenvectors $u_{G,i}$ but instead in terms of the corresponding eigenvalues³

via $\hat{g}(\Lambda_G) = \begin{pmatrix} \hat{g}(\lambda_{G,1}) & & \\ & \ddots & \\ & & \hat{g}(\lambda_{G,n}) \end{pmatrix}$. In order to learn such an eigenvalue filter $\hat{g} : \mathbb{R} \rightarrow \mathbb{R}$ via gradient descent, it requires some differentiable parameterization.

³ Here either the unnormalized eigenvalues of L_G or the eigenvalues of some normalized Laplacian, e.g. L_G^{sym} , can be used.

Chebyshev filters One such parameterization is based on the family of recursively defined Chebyshev polynomials $T_k(x) = 2xT_{k-1}(x) - T_{k-2}(x)$ with $T_0 = 1$ and $T_1 = x$ [Def+16]. It describes a spectral filter as a linear combination $\hat{g}_\theta(\lambda) := \sum_{k=0}^{K-1} \theta_k T_k(\lambda)$ with $\theta \in \mathbb{R}^K$. This restricts \hat{g}_θ to be a polynomial which allows us to rewrite the graph convolution from eq. (2.9) as

$$g_\theta * x_{G,j} = U_G^\top \hat{g}_\theta\left(\frac{2}{\max \lambda_G} \Lambda_G - I\right) U_G x_{G,j} = \hat{g}_\theta\left(\frac{2}{\max \lambda_G} L_G - I\right) x_{G,j} \quad (2.10)$$

because $L_G = U_G^\top \Lambda_G U_G$ is an eigendecomposition of the Laplacian. The $\frac{2}{\max \lambda_G} \Lambda_G - I$ term normalizes the eigenvalues to $[-1, 1]$ which prevents vanishing and exploding gradients. The advantage of this formulation is that it can be evaluated without actually having to compute the expensive eigendecomposition of L_G . Instead, by interpreting \hat{g}_θ as a matrix polynomial, one only has to compute the powers L_G^1, \dots, L_G^{K-1} and the largest eigenvalue $\max \lambda_G$ which is generally much cheaper than computing the full spectrum.

Linear filters Kipf and Welling [KW17] simplify the Chebyshev filter from eq. (2.10) even further in the ambiguously named *graph convolutional network* (GCN) architecture⁴. By fixing $K = 2$, by using a single filter parameter $\theta \in \mathbb{R}$ and by assuming that $\max \lambda_G^{\text{sym}} \approx 2$ (see definition 2.21, page 15) the convolution operation is reduced to

$$g_\theta * x_{G,j} = \theta \left(\tilde{D}_G^{-\frac{1}{2}} \tilde{A}_G \tilde{D}_G^{-\frac{1}{2}} \right) x_{G,j} \quad \text{with } \tilde{A}_G = A_G + I \text{ and } \tilde{D}_G = D_G + I. \quad (2.11)$$

In this formulation the spectral filter is effectively just a linear function $\hat{g}_\theta(\lambda) = \theta\lambda$. Via this simplified notion of convolution for a single feature signal $x_{G,j}$, a convolutional neural network layer over all features $\{x_{G,j}\}_{j=1}^d$ can analogously be defined as

$$Z^{(t)} := \sigma \left(\hat{A} Z^{(t-1)} \Theta^{(t)} \right) \quad \text{with } \hat{A} := \tilde{D}_G^{-\frac{1}{2}} \tilde{A}_G \tilde{D}_G^{-\frac{1}{2}} \quad \text{and} \quad Z^{(0)} := X_G. \quad (2.12)$$

Here σ is some non-linearity, e.g. ReLU, and $\Theta^{(t)} \in \mathbb{R}^{d^{(t-1)} \times d^{(t)}}$ is a matrix of learned filter parameters. This type of convolutional layer takes a graph signal $Z^{(t-1)} \in \mathbb{R}^{n \times d^{(t-1)}}$ and the corresponding adjacency matrix $A_G \in \mathbb{R}^{n \times n}$ as input and outputs a convolved signal $Z^{(t)} \in \mathbb{R}^{n \times d^{(t)}}$. By stacking multiple of those convolutional layers, complex non-linear signal filters can be learned despite the linearity of the underlying spectral filter.

⁴ We use “GCN” to refer to their proposed specific method in order to be consistent with other literature. We use “GCNN” to refer to the broader family of graph convolutional neural network methods.

Spatial GCNNs

Looking at the GCN layer defined in eq. (2.12), notice that, even though it is motivated by spectral graph theory, the spectrum λ_G is not actually directly used. This allows for a very different perspective on GCNs: Instead of interpreting convolutions as applications of linear spectral filters, we can interpret them as vertex neighborhood aggregations, similar to 1-WL. From this perspective a GCN can be seen as a so-called spatial GCNN because it operates directly in the vertex domain. To see why this is the case, we rewrite eq. (2.12) and compare it with the 1-WL color refinement strategy (see definition 2.9, page 8):

$$\text{GCN: } Z^{(t)}[v] = \sigma \left(\left(c(v)^2 Z^{(t-1)}[v] + \sum_{u \in \Gamma_G(v)} c(v)c(u) Z^{(t-1)}[u] \right) \Theta^{(t)} \right)$$

$$\text{1-WL: } \chi_{G,1}^{(t)}(v) = h \left(\chi_{G,1}^{(t-1)}(v), \{ \chi_{G,1}^{(t-1)}(u) \mid u \in \Gamma_G(v) \} \right)$$

Here $c(v) := (|\Gamma_G(v)| + 1)^{-\frac{1}{2}}$ are normalization factors introduced by $\tilde{D}_G^{-\frac{1}{2}}$. The comparison shows that GCN convolutions can be understood as iterative refinements of continuous “color vectors” $Z^{(t)}[v] \in \mathbb{R}^{d^{(t)}}$. Then the continuous analogue to the injective 1-WL hash function $h : \mathcal{C}^* \rightarrow \mathcal{C}$ can be defined as $h_{\text{GCN}}(z_0, z_1, \dots, z_m) = \sigma(\sum_{j=0}^m c(v_0)c(v_j)z_j \Theta^{(t)})$ which computes a single color vector from multiple color vectors z_j where v_j are the corresponding vertices.

A 1-WL bound on GNN power The relation between GCNNs using neighborhood aggregation convolution and 1-WL was formally analyzed by Xu et al. [Xu+19]. They show that the discriminative power of such a GCNN is upper-bounded by that of 1-WL. In particular the GCN architecture is strictly less powerful than 1-WL due to the fact that h_{GCN} is not an injective hash function. To overcome this limitation an alternative neighborhood aggregation architecture called *graph isomorphism network* (GIN) was proposed:

$$Z^{(t)}[v] := \text{MLP}^{(t)} \left(Z^{(t-1)}[v] + \sum_{u \in \Gamma_G(v)} Z^{(t-1)}[u] \right) \quad (2.13)$$

By leaving out the normalization factors $c(v)$ and by using a MLP instead of the single fully-connected layer $\sigma \circ \Theta^{(t)}$ the resulting hashing function $h_{\text{GIN}}(z_1, \dots, z_m) = \text{MLP}^{(t)}(\sum_{j=1}^m z_j)$ becomes injective⁵, i.e. it assigns a unique color vector to each multiset of color vectors. It was shown that this implies that GIN has the same discriminative power as 1-WL. As expected, GIN therefore fits training data better than non-injective GCNNs like GCN. Interestingly GIN additionally seems to generalize

⁵ Under the assumption that the set of possible input feature matrices $X \in \mathbb{R}^{n \times d^{(0)}}$ is countable. This is reasonable since real-world GC/GR domains typically only have a finite set of possible vertex feature vectors, e.g. one-hot label encodings.

better on test data than non-injective methods [Xu+19][Err+20]. It is not yet fully understood why this is the case.

Higher dimensional WL GNNs The majority of GNN methods uses a neighborhood aggregation scheme which limits their discriminative and, more importantly, computational power to that of 1-WL (see definition 2.16, page 11). To go beyond the limits of 1-WL, Morris et al. [Mor+19] proposed the first GCNN architecture inspired by the higher dimensional k -WL algorithms. Similar to the k -LWL kernel which we looked at in section 2.3.2, their so-called k -GNN uses the k -multiset and neighborhood localization optimizations to keep runtime costs feasible. The k -GNN convolution is described by

$$Z^{(t)}[s] := \sigma \left(Z^{(t-1)}[s]W^{(t)} + \sum_{v \in s, u \in \Gamma_G(v)} Z^{(t-1)}[s \setminus \{v\} \cup \{u\}]W_\Gamma^{(t)} \right). \quad (2.14)$$

It convolves the feature vectors of k -multisets $s \subseteq \mathcal{V}_G$ instead of single vertices $v \in \mathcal{V}_G$. Apart from this fundamental difference to 1-WL bounded GNNs, k -GNNs additionally use two learnable parameter matrices $W^{(t)}, W_\Gamma^{(t)} \in \mathbb{R}^{d^{(t-1)} \times d^{(t)}}$ instead of the single $\Theta^{(t)}$ used in GCNs. This separation of the parameter matrix effectively fulfills the same purpose as the MLP in GIN; it makes the implicitly defined k -GNN hash function injective. This can be seen by realizing that a stack of k -GNN convolution layers with $W_\Gamma^{(t)} = 0$ for all but the first layer simulates a MLP.

As a final remark, note that the concept of “neighborhood” in eq. (2.14) is slightly different from that used by the k -WL algorithm (see definition 2.10, page 9): k -GNN considers a single k -multiset as a neighbor while k -WL uses k -sets of k -multisets as neighbors. We will get back to this difference later.

Graph Pooling

The graph convolution approaches that we just looked at all produce a set of convolved feature vectors $\{Z^{(T)}[s_i]\}_{i=1}^m$ after T convolutional layers. For 1-WL bounded architectures like GCN or GIN, there is one vector for each of the $m = |\mathcal{V}_G|$ vertices, while a k -WL inspired architecture like k -GNN produces $m \leq |\mathcal{V}_G|^k$ output vectors. In order to solve the GC/GR problem, those vector sets need to be combined into a final predicted class or regression value. To do this, so-called *graph pooling layers* are used. Generally speaking there are two types of pooling approaches:

- 1. Hierarchical Pooling:** This type of pooling is similar to that found in CNNs on pictures where the resolution is iteratively reduced. Similarly hierarchical graph pooling iteratively *coarsens* a graph every couple of convolutional layers. Graph coarsening works by merging vertices in a spectrum-preserving manner [LV18].

This is done until a single merged vertex is left whose feature vector then represents the entire graph.

2. **Global Pooling:** Alternatively pooling can also be performed in a single step after the convolutional layers. This type of pooling takes all m feature vectors and directly maps them to a single graph feature vector.

In this thesis we will focus on global pooling. The most simple global pooling approaches use static aggregation functions like component-wise min, max or mean to produce a single graph feature vector $z_G \in \mathbb{R}^{d(L)}$. This vector is then fed into a standard MLP to produce the final prediction. The state-of-the-art graph pooling approaches go beyond static aggregation and try to incorporate structural information. We will now briefly look at two such approaches.

SortPooling One way to combine feature vectors is called *SortPooling* [Zha+18]. It interprets the convolved vectors as continuous WL colors that encode different structural roles of vertices (or vertex sets in case of k -GNNs). By imposing a component-wise lexicographic ordering on the set of color vectors, it can be reduced to a vertex permutation invariant top- p list of vectors (z_1, \dots, z_p) for some fixed $p \in \mathbb{N}$. The final graph feature vector then is the concatenation $z_G = (\bigoplus_{i=1}^p z_i) \in \mathbb{R}^{d(L)p}$. SortPooling is based on the idea that the convolutional layers will learn to use the most-significant lexicographic vector components to represent that vector's importance.

SAGPooling Another global pooling approach uses self-attention to explicitly assign a structural importance score to each vertex (or vertex set in case of k -GNNs). The so-called *self-attention graph pooling* (SAGPooling) [Lee+19] learns those attention scores via a separate stack of convolutional layers. The set of convolved feature vectors is then filtered down from the size m to $p = \lceil rm \rceil$ with $r \in [0, 1]$ by removing the vectors of the vertices with the lowest attention scores. Let z_1, \dots, z_p be the remaining feature vectors. To obtain the final graph feature vector, SAGPooling uses $z_G = (\sum_{i=1}^p z_i) \oplus \max_{i=1}^p z_i$.

Learning to Aggregate on Graphs

In the previous chapter an introduction to two separate fields of research was given: 1. *Learning to aggregate* (LTA), 2. *Graph classification and regression* (GC/GR). In this chapter we will combine them and define an extension of LTA to the GC/GR problem. This will be done in three steps:

1. We begin with a formal definition of what actually constitutes an LTA method as opposed to non-LTA methods.
2. Using this definition, we will see that some of the previously described GC/GR methods can be interpreted as LTA variants under certain conditions.
3. Finally a novel LTA-inspired GCNN architecture will be described.

3.1 A Generalized Definition of LTA

In order to formally define LTA, we must first decide on its defining characteristic. We propose that this characteristic should be the *localized explainability* of LTA predictions. As seen in section 2.1, an LTA score $y_C \in \mathcal{Y}$ for some multiset composition $C = \{c_1, \dots, c_n\}$ can always be tracked back to a set of local constituent scores $y_1, \dots, y_n \in \mathcal{Y}$. Under the assumption that each constituent c_i represents some human interpretable object, a composition's score y_C can therefore be explained by the presence of certain indicative constituents/objects c_i .

Based on this intuition we now give a generalized definition of LTA which applies to unstructured as well as structured input data. We assume that all compositions are represented by graphs $G \in \mathcal{G}$; an unstructured input is represented by a graph with one vertex per constituent ($\mathcal{V}_G = \{v_{c_1}, \dots, v_{c_n}\}$) and no edges ($\mathcal{E}_G = \emptyset$). Each composition has some target score $y_G \in \mathcal{Y}$ which could be a discrete class or continuous value. An *LTA model* $h : \mathcal{G} \rightarrow \mathcal{Y}$ assigns predictions $\hat{y}_G \in \mathcal{Y}$ to compositions G which ideally correspond to the true score y_G . Such a model must satisfy three criteria:

1. **Decomposition:** A given composition G must be decomposed into a set of constituents $c_{G,i}$ via a *decomposition function* $\psi : \mathcal{G} \rightarrow \mathcal{P}(\mathcal{G})$.

Definition 3.1. ψ is a *decomposition function* iff. it splits a graph into a subset of its subgraphs, i.e. $\forall G \in \mathcal{G} : \forall c_{G,i} \in \psi(G) : \exists s \in \mathcal{P}(\mathcal{V}_G) : c_{G,i} = G[s]$.

Note that the strict equality $c_{G,i} = G[s]$ is used in definition 3.1 instead of just requiring subgraph isomorphism ($c_{G,i} \simeq G[s]$) because a constituent $c_{G,i}$ represents a specific localized subgraph of a structured composition.

In the existing unstructured LTA approaches the decomposition function is implicitly defined as $\psi(G) := \{G[v_{c_i}]\}_{v_{c_i} \in \mathcal{V}_G}$ since each vertex v_{c_i} corresponds to an interpretable constituent c_i by definition. For structured data however, a split into individual vertices is typically not appropriate. Molecular graphs from chemical datasets for example are meaningfully characterized by the presence of so-called *functional groups* consisting of multiple bonded atoms while a characterization on the level of individual atoms is generally less meaningful [MW97].

2. **Local evaluation:** The constituents $c_{G,i} \in \psi(G)$ must be evaluated via some function $f : \mathcal{G} \rightarrow \mathcal{Y} \times \mathbb{R}$. This *evaluation function* assigns a prediction $\hat{y}_{G,i} \in \mathcal{Y}$ and a weight $w_{G,i} \in \mathbb{R}$ to each constituent. A constituent's weight $w_{G,i}$ can intuitively be interpreted as a measure of the confidence that the local prediction $\hat{y}_{G,i}$ is indicative of the composition's global target score y_G . Learning local predictions and weights for all possible constituents is called the *disaggregation problem*.

Note that there are no explicit constituent weights in the existing unstructured LTA approaches (i.e. implicitly all $w_{G,i} = 1$) because the explicitly given constituents are assumed to be equally indicative of y_G . For structured data however, where the decomposition $\psi(G)$ is not given as part of the input, this assumption does not necessarily hold. By weighting the constituents, an LTA model can reduce the relevance or even ignore constituents that turn out to be irrelevant for the compositions target score y_G .

3. **Aggregation:** Lastly a *weighted aggregation function* $\mathcal{A} : (\mathcal{Y} \times \mathbb{R}_{\geq 0})^* \rightarrow \mathcal{Y}$ must be applied. It combines the multiset of local constituent predictions and non-negative weights into a single global composition prediction.

Definition 3.2. We call \mathcal{A} a *weighted aggregation function* iff. it satisfies

$$\begin{aligned} \text{idempotency: } & \exists \eta > 0 : \forall y \in \mathcal{Y}, w \in \mathbb{R}_{\geq 0}^n \text{ s.t. } \max w \geq \eta : \mathcal{A}(\{(y, w_i)\}_{i=1}^n) = y \\ \wedge \text{zero invar.: } & \forall y_0 \in \mathcal{Y}, S = \{(y_i, w_i)\}_{i=1}^n : \mathcal{A}(S \cup \{(y_0, 0)\}) = \mathcal{A}(S). \end{aligned}$$

The idempotency constraint requires aggregation functions to agree with uniform input scores y if at least one input is weighted above some threshold η . The zero invariance constraint requires aggregation functions to ignore inputs with zero weight. Exemplary weighted aggregation function are:

- The *weighted mean* function $\text{wmean}(\{(y_i, w_i)\}_{i=1}^n) := \sum_{i=1}^n w_i y_i$ which

requires $\sum w_i = 1$, $w_i \in [0, 1]$ and the existence of some scalar multiplication operator $\cdot : \mathbb{R} \times \mathcal{Y} \rightarrow \mathcal{Y}$, typically from some subfield $\mathcal{Y} \subseteq \mathbb{R}$ or possibly also some vector subspace $\mathcal{Y} \subseteq \mathbb{R}^d$.

- Another basic weighted aggregator is the *weighted majority vote* function $\text{wmaj}(\{(y_i, w_i)\}_{i=1}^n) := \arg \max_{y \in \mathcal{Y}} \sum_{y_i=y} w_i$ which returns the input with the highest total weight. Unlike wmean it can also be applied to score domains \mathcal{Y} without a multiplication operator, e.g. sets of discrete classes.
- Alternatively an unweighted aggregation function like min, max, mean or OWA¹ also trivially satisfies definition 3.2 if all inputs y_i with $w_i = 0$ are filtered out and the weights for all remaining inputs are ignored.

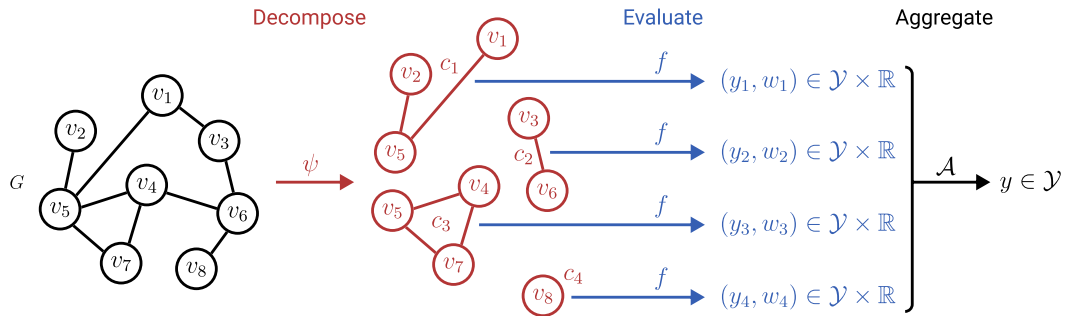


Figure 3.1. Overview of the generalized LTA architecture for structured data.

Based on the notion of decomposition, local evaluation and aggregation we can now define the concept of *LTA formulations*.

Definition 3.3. A model $h : \mathcal{G} \rightarrow \mathcal{Y}$ is in an *LTA formulation* iff. it is expressed as

$$h(G) := \mathcal{A}(\{f(c_{G,i}) \mid c_{G,i} \in \psi(G)\}) \quad \text{with } \psi, f \text{ and } \mathcal{A} \text{ as defined above.}$$

Note that every model $h : \mathcal{G} \rightarrow \mathcal{Y}$ has a trivial recursive LTA formulation by choosing $\psi(G) = \{G\}$, $f(G) = (h(G), 1)$ and an arbitrary weighted aggregation function \mathcal{A} . Those trivial LTA formulations do not split compositions into locally evaluated constituents and therefore intuitively do not fulfill the postulated localized explainability characteristic of LTA. However since there is no commonly accepted formal criterion to decide whether a model's decisions are explainable [Lip18], we do not attempt to strictly distinguish between LTA and non-LTA methods. Instead the notion of LTA formulations should be seen as way to identify how "LTA-like" a model is:

- **Negative extreme:** If a model h only has trivial LTA formulations with the decomposition function $\psi(G) = \{G\}$, it is not considered to be an LTA model.

¹ Even though OWA uses weights, it does not get those weights as part of the input and is therefore considered to be unweighted in this context.

- **Positive extreme:** If a model has an LTA formulation with a decomposition function that returns interpretable constituents, it is considered to be an LTA model. By definition this is true for the single-vertex constituents $\psi(G) := \{G[v_{c_i}]\}_{v_{c_i} \in \mathcal{V}_G}$ of LTA methods for unstructured data.
- **In-between cases:** An LTA method for structured data must produce models that lie somewhere in-between the two extremes.

The more “LTA-like” a given model is, the stronger its bias towards locally explainable predictions, which in turn reduces the potential expressive power of the model. Gilpin et al. [Gil+18] describe this trade-off between explainability and expressive power in more detail. However, when considering problem domains in which the true composition scores y_G are accurately described by an LTA-like generative process, a less expressive LTA-like model could generalize better than a more expressive non-LTA model. This idea is captured by the so-called *LTA assumption*.

Definition 3.4. A problem domain \mathcal{D} satisfies the *LTA assumption* iff. there is an LTA method which produces models with an equal or lower out-of-sample error than the models produced by non-LTA methods for most training samples $\mathcal{D}_{\text{train}} \subseteq \mathcal{D}$.

Due to the fuzziness of the class of LTA methods, the LTA assumption is naturally also a fuzzy concept. Nonetheless evidence for its truthiness in a given domain \mathcal{D} can be empirically obtained by comparing candidate LTA methods with the best known non-LTA method for \mathcal{D} , assuming that some cut-off condition for the required “LTA-ness” of an LTA method is agreed upon.

3.2 LTA Formulations of Existing GC/GR Methods

Based on the general definition of LTA from the last section, we will now see to what extent the GC/GR methods described in section 2.3 can be interpreted as LTA instances. First the relation between SVMs on graph embeddings and LTA will be explored. Then we will provide an LTA perspective on GCNNs.

3.2.1 SVMs on Graph Embeddings as LTA Models

In sections 2.3.1 and 2.3.2 three different ways to map a given graph G to a vector $\varphi(G) \in \mathbb{R}^d$ were described: 1. Fingerprint embeddings, 2. skip-gram inspired embeddings and 3. kernel embeddings. One common way to solve the GC/GR problem via those embedding vectors is to train an SVM on them. We will now see that SVMs can be interpreted as LTA models if they are trained on so-called *substructure component embeddings* (SSCEs).

Definition 3.5. Given a multiset $A = \{\!\{ \underbrace{a_1, \dots, a_1}_{\gamma_A(a_1) \text{ times}}, \dots, \underbrace{a_n, \dots, a_n}_{\gamma_A(a_n) \text{ times}} \}\!\} \subseteq D$, the so-called *multiplicity function* $\gamma_A : D \rightarrow \mathbb{N}_0$ maps each element of the domain D to its multiplicity in A with $\gamma_A(x) = 0 \Leftrightarrow x \notin A$.

Definition 3.6. A graph embedding $\varphi : \mathcal{G} \rightarrow \mathbb{N}_0^d$ is called a *substructure component embedding* (SSCE) iff. there are decomposition functions $\psi_{\varphi,i} : \mathcal{G} \rightarrow \mathcal{P}(\mathcal{G})$ and multiplicity functions $\gamma_{\varphi,i} : \mathcal{G} \rightarrow \mathbb{N}_0$ for all embedding components $i \in [d]$ s.t. $\forall G \in \mathcal{G}, i \in [d] : \varphi(G)[i] = \sum_{c \in \psi_{\varphi,i}(G)} \gamma_{\varphi,i}(c)$ where $\gamma_{\varphi,i}$ is the multiplicity function of a multiset of the constituents $\psi_{\varphi,i}(G)$. We call $\psi_{\varphi,i}$ an *underlying decomposition* of the i -th component of the embedding φ . Similarly the joint decomposition $\psi_{\varphi}(G) := \bigcup_{i=1}^d \psi_{\varphi,i}(G)$ is an *underlying decomposition* of φ .

Intuitively definition 3.6 states that the value of each SSCE component must be derived from the number of constituents produced by some decomposition function where each constituent might be counted multiple times. Based on this requirement we now proof the main theorem which shows the relation between SVMs and LTA.

Theorem 3.7. A binary SVM graph classifier h that applies a SSCE φ to its inputs has an LTA formulation that uses an underlying decomposition ψ_{φ} of φ .

Proof. Let $h : \mathcal{G} \rightarrow \{-1, +1\}$ be a binary graph classifier expressed as $h = h_{\text{SVM}} \circ \varphi$ where $\varphi : \mathcal{G} \rightarrow \mathbb{N}_0^d$ is an SSCE and $h_{\text{SVM}} : \mathbb{R}^d \rightarrow \{-1, +1\}$ a standard SVM classifier. Additionally, let ψ_{φ} be some underlying decomposition of φ with $\{\gamma_{\varphi,i}\}_{i=1}^d$ being the corresponding multiplicity functions.

Based on this decomposition we now bring the SVM graph classifier h into an LTA formulation. If h is trained on a dataset $\mathcal{D}_{\text{train}} = \{(G_1, y_1), \dots, (G_N, y_N)\}$, via the kernel trick it can be expressed as

$$\begin{aligned} h(G) &= \text{sgn} \left(\sum_{j=1}^N \alpha_j y_j \langle \varphi(G), \varphi(G_j) \rangle + b \right) \quad \text{for some } \alpha \in \mathbb{R}_{\geq 0}^N \text{ and } b \in \mathbb{R} \\ &= \text{sgn} \left(\sum_{i=1}^d \varphi(G)[i] \underbrace{\left(\sum_{j=1}^N \alpha_j y_j \varphi(G_j)[i] \right)}_{\beta_i} + b \right) = \text{sgn} \left(\sum_{i=1}^d \varphi(G)[i] \beta_i + b \right) \\ &= \text{sgn} \left(\sum_{c_t \in \psi_{\varphi}(G)} \underbrace{\sum_{i=1}^d \gamma_{\varphi,i}(c_t) \beta_i}_{z_t} + b \right) = \text{sgn} \left(\sum_{c_t \in \psi_{\varphi}(G)} \underbrace{|z_t|}_{w_t} \underbrace{\text{sgn } z_t}_{y_t} + \underbrace{|b|}_{w_b} \underbrace{\text{sgn } b}_{y_b} \right) \\ &= \text{wmaj} (\{(y_t, w_t) \mid c_t \in \psi_{\varphi}(G)\} \cup \{(y_b, w_b)\}). \end{aligned}$$

By choosing $f_h(c_t) := (y_t, w_t)$ and $\mathcal{A}_h(S) = \text{wmaj}(S \cup \{(y_b, w_b)\})$, the SVM model therefore has an LTA formulation with the decomposition function ψ_{φ} .

To complete the proof it now remains to show that f_h and \mathcal{A}_h are in fact a local evaluation function and a weighted aggregation function respectively. To see that f_h perform local evaluation, note that $f_h(c_t) := (\text{sgn } z_t, |z_t|)$ with $z_t := \sum_{i=1}^d \gamma_{\varphi,i}(c_t) \beta_i$ only depends on the shared multiplicity functions $\gamma_{\varphi,i}$, the constants β_i and the constituent c_t ; apart from c_t no other information from the input graph G is required by f_h which makes it a local evaluation function. To see why \mathcal{A}_h satisfies definition 3.2, note that it inherits the idempotency property from wmaj because \mathcal{A}_h ignores the bias “pseudo-constituent” (y_b, w_b) for all threshold weights $\max w_t \geq \eta > w_b$, similarly the zero invariance of wmaj is also directly inherited. This concludes the proof. \square

The central statement of theorem 3.7 is that SVM graph classifiers that use an SSCE φ implicitly perform an LTA-like weighted majority vote aggregation of constituent scores y_t . Those constituent scores can in turn be expressed as a majority vote of the graph scores in the training dataset $\mathcal{D}_{\text{train}}$:

$$\begin{aligned} y_t := \text{sgn } z_t &= \text{sgn} \left(\sum_{j=1}^N \underbrace{\left(\alpha_j \sum_{c_k \in \psi_{\varphi}(G_j)} \sum_{i=1}^d \gamma_{\varphi,i}(c_t) \gamma_{\varphi,i}(c_k) \right) y_j}_{w_j} \right) \\ &= \text{wmaj}(\{(y_j, w_j) \mid j \in [N]\}) \end{aligned} \quad (3.1)$$

Note that, if the constituents of G_j all come from different embedding components than those of G ($\forall i \in [d] : \psi_{\varphi,i}(G_j) \cap \psi_{\varphi,i}(G) = \emptyset$), then G_j has no influence on the score of G ($w_j = 0$).

To see what theorem 3.7 implies in practice, we will now apply it to the graph embedding approaches described in sections 2.3.1 and 2.3.2:

- 1. Fingerprint embeddings:** Here the i -th embedding component represent the number of occurrences of a substructure S_i , i.e. $\varphi_{\text{FP}}(G)[i] := \text{count}_{S_i}(G)$ (see definition 2.16, page 11). Such a fingerprint embedding naturally is an SSCE with the decomposition functions $\psi_{\text{FP},i}(G) := \{G[\text{set}(s)] \mid s \in \mathcal{V}_G^* \wedge G[s] \equiv S_i\}$ and the multiplicity functions $\gamma_{\text{FP},i}(c) := \mathbb{1}[c \simeq S_i]$ since those functions produce the subgraphs that are counted by $\varphi_{\text{FP}}(G)[i]$ with multiplicity 1.

Under the assumption that the substructure patterns S_i are chosen s.t. the their instances $c \in \psi_{\text{FP},i}(G)$ are nontrivial interpretable constituents, the underlying joint decomposition $\psi_{\text{FP}}(G) := \bigcup_{i=1}^d \psi_{\text{FP},i}(G)$ must also be nontrivial and interpretable. Thus, by theorem 3.7, SVMs trained on fingerprint embeddings are LTA models that produce locally explainable predictions. LTA

- 2. graph2vec:** The skip-gram inspired graph2vec embedding produces vectors $\varphi(G) \in \mathbb{R}^d$ whose individual components do not have a clear interpretation. graph2vec embeds graphs that have common 1-WL colors closer to each other

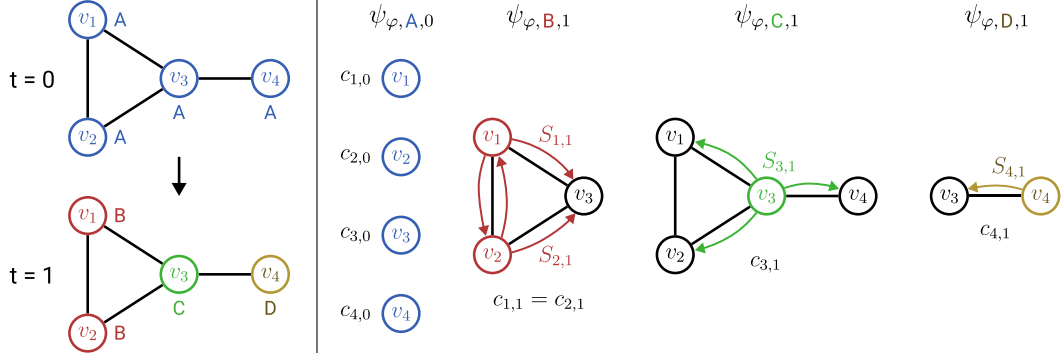


Figure 3.2. The constituents $c_{j,t}$ implied by the WL subtree embedding vector $\varphi(G) = (\underbrace{4, 0, 0, 0}_{t=0}, \underbrace{0, 2, 1, 1}_{t=1})$. The subtrees $S_{j,t}$ that span each constituent $c_{j,t}$ are visualized by the colored arrows that originate from the colored root vertices. Because $S_{1,1}$ and $S_{2,1}$ span the same constituent $c = c_{1,1} = c_{2,1} = G[\{v_1, v_2, v_3\}]$, its multiplicity is $\gamma_{\varphi, B, 1}(c) = 2$; the multiplicity of all other constituents is 1.

than graphs that do not share the same colors (see eq. (2.5), page 18). The resulting component values can be arbitrary reals, therefore this approach is not an SSCE which in turn implies that it does not have an LTA formulation as in theorem 3.7. non-LTA

3. WL subtree kernel: The individual components of the WL subtree kernel's embedding φ_{ST} represent the number of occurrences of a color $\kappa_i \in \mathcal{C}$, i.e. $\varphi_{ST}(G)[i, t] := dist_{\chi_{G,1}^{(t)}}(\kappa_i)$ as defined in eq. (2.6) on page 18². The occurrence of a color κ_i at some vertex $v_j \in \mathcal{V}_G$ in the t -th refinement step (i.e. $\chi_{G,1}^{(t)}(v_j) = \kappa_i$) in turn implies that the *breadth-first-search* (BFS) tree $S_{j,t} := \text{BFS}(G, v_j, t)$ of depth t rooted at v_j is isomorphic to some WL color subtree S_{κ_i} (i.e. $S_{j,t} \simeq S_{\kappa_i}$). This relation between WL colors κ_i and subtrees S_{κ_i} was illustrated in fig. 2.10 on page 19.

To show that φ_{ST} is an SSCE, we have to define decomposition functions $\psi_{\varphi,i,t}$ and multiplicity functions $\gamma_{\varphi,i,t}$ s.t. $\varphi(G)[i, t] = \sum_{c \in \psi_{\varphi,i,t}(G)} \gamma_{\varphi,i,t}(c)$. Since $\varphi(G)[i, t]$ counts the occurrences $S_{j,t}$ of a subtree S_{κ_i} in G , the SSCE requirement would be trivially satisfied if each $S_{j,t}$ were a constituent with multiplicity 1. This intuition is however not quite correct because the constituents of a graph G must be induced subgraphs of G , not BFS subtrees $S_{j,t}$ of G .

To fix the previous intuition we “convert” the subtrees $S_{j,t}$ into proper subgraph constituents via $c_{j,t} := G[V_{S_{j,t}}]$, i.e. the subgraphs that are spanned by the subtrees. The resulting decomposition functions are $\psi_{\varphi,i,t}(G) := \{c_{j,t} \mid v_j \in \mathcal{V}_G \wedge S_{j,t} \simeq S_{\kappa_i}\}$. As illustrated in fig. 3.2, the number of distinct constituents $c_{j,t}$ might be smaller than the number of BFS subtrees $S_{j,t}$ because two distinct subtrees might span the same set of vertices. To fix this discrepancy between

² To avoid confusion $\kappa_i \in \mathcal{C}$ is used for colors and $c_j \in \mathcal{G}$ for constituents in this context.

the subtree occurrence count (which equals $\varphi(G)[i, t]$) and the number of constituents, the multiplicities $\gamma_{\varphi, i, t}(c)$ of the constituents c have to correspond to the number of BFS subtrees they were spanned up by, i.e.

$$\gamma_{\varphi, i, t}(c) := |\{S = \text{BFS}(c, v_{\text{root}}, t) \mid v_{\text{root}} \in \mathcal{V}_c \wedge S \simeq S_{\kappa_i} \wedge \text{complete}(S)\}|$$

with $\text{complete}(S) \Leftrightarrow \forall \text{ leaf nodes } v_{\text{leaf}} \text{ of the tree } S : |\Gamma_c(v_{\text{leaf}})| = |\Gamma_G(v_{\text{leaf}})|$.

The purpose of the $\text{complete}(S)$ condition is to only count the BFS subtrees of the constituent c that are also BFS subtrees of the complete graph G . To see why this is required, note that in fig. 3.2 the $c_{1,1}/c_{2,1}$ constituent contains the color subtree S_B three times (rooted at v_1 , v_2 and v_3) even though G only contains it twice (rooted at v_1 and v_2). Also note that, since $\gamma_{\varphi, i, t}(c)$ must only depend on a given constituent c and not on the graph G it was decomposed from, the degree information $|\Gamma_G(v_{\text{leaf}})|$ of the constituent vertices $v \in \mathcal{V}_c$ is assumed to be statically encoded in the labels $l_c[v]$ or feature vectors $x_c[v]$.

Via the decomposition and multiplicity functions that were just described, φ_{ST} is in fact an SSCE with a nontrivial, subtree-based decomposition function. Additionally each constituent's diameter is upper bounded by $2T$ (with T being the maximum number of WL iterations) which guarantees that constituents are localized within a neighborhood of bounded size. By theorem 3.7, SVMs that use the WL subtree kernel therefore have nontrivial LTA formulations with localized constituents, i.e. they can be considered to be “LTA-like” models. However, unlike fingerprint embeddings, the WL subtree constituents are not manually chosen to be interpretable. This implies that the localized explainability characteristic of LTA is only partially satisfied since the SVM predictions are based on local constituent predictions that are not necessarily interpretable.

LTA-like

- 4. WL shortest path kernel:** As defined in eq. (2.7) on page 19, the i -th component of the WL shortest path embedding φ_{SP} represents a 4-tuple $(t_i, a_i, b_i, d_i) \in \{0, \dots, T\} \times \mathcal{C} \times \mathcal{C} \times \mathbb{N}_0$. The value $\varphi_{\text{SP}}(G)[i]$ is defined as the number of vertex pairs $v_a, v_b \in \mathcal{V}_G$ that have a shortest connecting path of length d_i and the WL color combination $\chi_{G,1}^{(t_i)}(v_a) = a_i$ and $\chi_{G,1}^{(t_i)}(v_b) = b_i$.

To determine the number of such vertex pairs via an SSCE multiplicity function $\gamma_{\varphi, t_i, a_i, b_i, d_i}$, each connected pair of vertices v_a, v_b and the shortest path between them must occur together in at least one constituent, otherwise a multiplicity function cannot compute whether v_a and v_b are in fact d_i hops apart. One simple decomposition which guarantees that all shortest paths are part of at least one constituent simply splits a given graph into its connected components. Even though such a decomposition is non-trivial since it uses at least some structural information to determine the set of constituents, the fact that any

pair of connected vertices must co-occur within a single constituent means that constituents must span arbitrarily large distances within a given graph. Depending on ones domain-specific interpretation of *localized explainability*, this restriction can be seen to be not “LTA-like”. Since we do not attempt to clearly separate LTA from non-LTA methods, φ_{SP} is categorized as an in-between case here.

partially LTA-like

5. **k -LWL kernel:** The LTA interpretation of the k -LWL kernel is identical to that of the WL subtree kernel. The WL color of a k -multiset of vertices s after t refinement steps is described by the joint t -neighborhood of all vertices $v \in s$, i.e. $\Gamma_G^t(s) := \bigcup_{v \in s} \Gamma_G^t(v)$. Analogous to WL subtree embeddings, those t -neighborhoods form the localized constituents of the k -LWL kernel via a BFS over neighboring k -multisets. Consequently SVMs using the k -LWL kernel can be interpreted as “LTA-like” methods with nontrivial localized decompositions.

LTA-like

6. **k -GWL kernel:** The only difference between the k -LWL and the k -GWL kernel is their definition of the k -multiset neighborhood. Namely the refined color of a multiset $s \subseteq \mathcal{V}_G$ in k -GWL depends on the colors of all vertices \mathcal{V}_G since all multisets $s' = s \setminus \{v\} \cup \{u\}$ with $v \in s$ and $u \in \mathcal{V}_G$ are neighbors of s . Because of those global multiset neighborhoods, all the color subtrees of a graph span the entire graph. Therefore the k -GWL embedding is an SSCE with only the trivial decomposition function $\psi_\varphi(G) = \{G\}$. Thus the LTA formulation of k -GWL SVMs described in theorem 3.7 is also trivial which means that they are not LTA models.

non-LTA

This concludes our overview of LTA interpretations of SVMs that use graph embeddings/kernels. Among the described approaches, fingerprint embeddings, the WL subtree kernel and the k -LWL kernel were shown to have LTA formulations with nontrivial local decomposition functions. Approaches like graph2vec, the WL shortest path kernel or k -GWL on the other hand, were shown to be less compatible with LTA.

3.2.2 GCNNs as LTA Models

Now we will look at the GCNN approaches described in section 2.3.3 from an LTA perspective. As described in the last section, SVMs can be interpreted as LTA methods if they use an SSCE embedding; similarly GCNNs also have LTA formulations under certain conditions that are described in this section.

While the SVM LTA formulation from theorem 3.7 uses a single fixed aggregation function, namely wmaj , the aggregation function in GCNN architectures can be chosen more freely. This is due to the fact that GCNNs have an LTA formulation in which

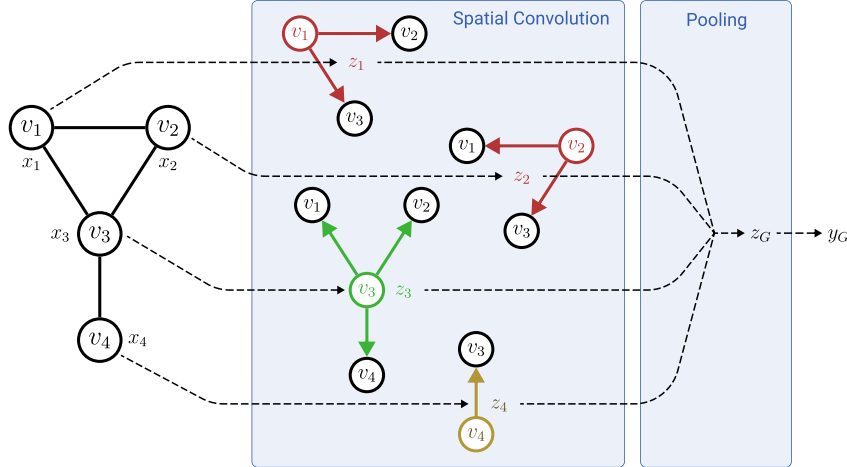


Figure 3.3. An LTA perspective on GCNNs that use vertex neighborhood convolutions.

the convolutional layers implicitly define the decomposition and local evaluation functions while the pooling layer directly corresponds to the LTA aggregation function. This correspondence is illustrated in fig. 3.3. As described in section 2.3.3, a stack of T vertex convolution layers computes a feature vector $z_i \in \mathbb{R}^{(T)}$ for all vertices $v_i \in \mathcal{V}_G$ of an input graph G . Depending on the specific type of convolutional layer, each of those feature vectors z_i is the result of some subset of the input feature vectors $\{x_i\}_{v_i \in \mathcal{V}_G}$:

1. Spectral convolutions with arbitrary filters:

- 2. Spatial vertex convolutions:** If the convolutional layers use a neighborhood aggregation scheme, the receptive field of vertices that have an influence on z_i is equal to the 1-WL subtree of v_i after T refinement steps as described by Xu et al. [Xu+19]. Similar to the WL subtree kernel, each $z_i \in \mathbb{R}^{(T)}$ can therefore be interpreted as the evaluation of a localized subtree.

3.3 A Novel LTA-Inspired GCNN Architecture

4

Evaluation

Conclusion

5.1 Review

5.2 Future Directions

Appendix

A

Bibliography

- [AB73] George W. Adamson and Judith A. Bush. „A method for the automatic classification of chemical structures“. In: *Information Storage and Retrieval* 9.10 (1973), pp. 561–568 (cit. on pp. 12, 16).
- [Alz+10] Alfredo Alzaga, Rodrigo Iglesias, and Ricardo Pignol. „Spectra of symmetric powers of graphs and the Weisfeiler–Lehman refinements“. In: *Journal of Combinatorial Theory, Series B* 100.6 (2010), pp. 671–682. arXiv: 0801 . 2322v1 [math.SP] (cit. on p. 14).
- [Arv+19] Vikraman Arvind, Frank Fuhlbrück, Johannes Köbler, and Oleg Verbitsky. „On Weisfeiler-Leman Invariance: Subgraph Counts and Related Graph Properties“. In: *Fundamentals of Computation Theory*. Springer International Publishing, 2019, pp. 111–125. arXiv: 1811.04801v3 [cs.DM] (cit. on p. 12).
- [Bab+80] László Babai, Paul Erdős, and Stanley M. Selkow. „Random graph isomorphism“. In: *SIAM Journal on computing* 9.3 (1980), pp. 628–635 (cit. on pp. 7, 11).
- [Bab15] László Babai. *Graph Isomorphism in Quasipolynomial Time*. Dec. 11, 2015. arXiv: 1512.03547v2 [cs.DS] (cit. on p. 7).
- [Ban+18b] Priyanka Banerjee, Andreas O. Eckert, Anna K. Schrey, and Robert Preissner. „ProTox-II: a webserver for the prediction of toxicity of chemicals“. In: *Nucleic Acids Research* 46.W1 (2018), W257–W263 (cit. on p. 16).
- [BK05] K.M. Borgwardt and H. Kriegel. „Shortest-Path Kernels on Graphs“. In: *Fifth IEEE International Conference on Data Mining (ICDM'05)*. IEEE, 2005 (cit. on p. 19).
- [Bru+13] Joan Bruna, Wojciech Zaremba, Arthur Szlam, and Yann LeCun. *Spectral Networks and Locally Connected Networks on Graphs*. Dec. 21, 2013. arXiv: 1312.6203v3 [cs.LG] (cit. on p. 21).
- [Cai+92] Jin-Yi Cai, Martin Fürer, and Neil Immerman. „An optimal lower bound on the number of variables for graph identification“. In: *Combinatorica* 12.4 (1992), pp. 389–410 (cit. on p. 7).
- [Chu10] Fan Chung. „Graph theory in the information age“. In: *Notices of the American Mathematical Society* 57 (June 2010) (cit. on p. 20).
- [Das04] K.Ch. Das. „The Laplacian spectrum of a graph“. In: *Computers & Mathematics with Applications* 48.5-6 (2004), pp. 715–724 (cit. on p. 14).

- [Def+16] Michaël Defferrard, Xavier Bresson, and Pierre Vandergheynst. „Convolutional Neural Networks on Graphs with Fast Localized Spectral Filtering“. In: *Proceedings of the 30th International Conference on Neural Information Processing Systems*. NIPS’16. Barcelona, Spain: Curran Associates Inc., 2016, pp. 3844–3852. arXiv: 1606.09375v3 [cs.LG] (cit. on p. 22).
- [Drw+14] Małgorzata N. Drwal, Priyanka Banerjee, Mathias Dunkel, Martin R. Wettig, and Robert Preissner. „ProTox: a web server for the in silico prediction of rodent oral toxicity“. In: *Nucleic Acids Research* 42.W1 (2014), W53–W58 (cit. on p. 16).
- [Err+20] Federico Errica, Marco Podda, Davide Bacci, and Alessio Micheli. „A Fair Comparison of Graph Neural Networks for Graph Classification“. In: *International Conference on Learning Representations*. ICLR’2020. 2020. arXiv: 1912.09893v2 [cs.LG] (cit. on p. 24).
- [Fü17] Martin Fürer. „On the Combinatorial Power of the Weisfeiler-Lehman Algorithm“. In: *Lecture Notes in Computer Science*. Springer International Publishing, 2017, pp. 260–271. arXiv: 1704.01023v1 [cs.DS] (cit. on p. 12).
- [GL16] Aditya Grover and Jure Leskovec. *node2vec: Scalable Feature Learning for Networks*. July 3, 2016. arXiv: 1607.00653v1 [cs.SI] (cit. on p. 17).
- [Gor+05] M. Gori, G. Monfardini, and F. Scarselli. „A new model for learning in graph domains“. In: *Proceedings. 2005 IEEE International Joint Conference on Neural Networks, 2005*. IEEE, 2005 (cit. on p. 20).
- [Gu+15] Jiao Gu, Bobo Hua, and Shiping Liu. „Spectral distances on graphs“. In: *Discrete Applied Mathematics* 190-191 (2015), pp. 56–74. arXiv: 1402.6041v2 [math.SP] (cit. on p. 14).
- [Hen+15] Mikael Henaff, Joan Bruna, and Yann LeCun. *Deep Convolutional Networks on Graph-Structured Data*. June 16, 2015. arXiv: 1506.05163v1 [cs.LG] (cit. on p. 21).
- [IL90] Neil Immerman and Eric Lander. „Describing graphs: A first-order approach to graph canonization“. In: *Complexity theory retrospective*. Springer, 1990, pp. 59–81 (cit. on pp. 11, 12).
- [Kek66] Aug. Kekulé. „Untersuchungen über aromatische Verbindungen. I. Ueber die Constitution der aromatischen Verbindungen.“ In: *Annalen der Chemie und Pharmacie* 137.2 (1866), pp. 129–196 (cit. on p. 12).
- [Kie+17] Sandra Kiefer, Ilia Ponomarenko, and Pascal Schweitzer. „The Weisfeiler-Leman dimension of planar graphs is at most 3“. In: *2017 32nd Annual ACM/IEEE Symposium on Logic in Computer Science (LICS)*. IEEE, 2017. arXiv: 1708.07354v1 [cs.DM] (cit. on p. 12).
- [Kri+20] Nils M. Kriege, Fredrik D. Johansson, and Christopher Morris. „A survey on graph kernels“. In: *Applied Network Science* 5.1 (2020). arXiv: 1903.11835v2 [cs.LG] (cit. on p. 18).
- [KW17] Thomas N. Kipf and Max Welling. „Semi-Supervised Classification with Graph Convolutional Networks“. In: *International Conference on Learning Representations* (2017). arXiv: 1609.02907v4 [cs.LG] (cit. on p. 22).

- [LB98] Yann LeCun and Yoshua Bengio. „Convolutional Networks for Images, Speech, and Time Series“. In: *The Handbook of Brain Theory and Neural Networks*. Cambridge, MA, USA: MIT Press, 1998, pp. 255–258 (cit. on p. 21).
- [Lee+19] Junhyun Lee, Inyeop Lee, and Jaewoo Kang. „Self-Attention Graph Pooling“. In: *Proceedings of the 36st International Conference on Machine Learning*. ICML’19. Apr. 17, 2019, pp. 6661–6670. arXiv: 1904.08082v4 [cs.LG] (cit. on p. 25).
- [Lip18] Zachary C. Lipton. „The Mythos of Model Interpretability“. In: *Queue* 16.3 (June 2018), 31–57. arXiv: 1606.03490v3 [cs.LG] (cit. on p. 29).
- [LM14] Quoc Le and Tomas Mikolov. „Distributed Representations of Sentences and Documents“. In: *Proceedings of the 31st International Conference on Machine Learning - Volume 32*. ICML’14. Beijing, China, 2014, pp. II–1188–II–1196. arXiv: 1405.4053v2 [cs.CL] (cit. on p. 18).
- [Lue+18] Thomas Luechtfeld, Dan Marsh, Craig Rowlands, and Thomas Hartung. „Machine Learning of Toxicological Big Data Enables Read-Across Structure Activity Relationships (RASAR) Outperforming Animal Test Reproducibility“. In: *Toxicological Sciences* 165.1 (2018), pp. 198–212 (cit. on p. 16).
- [LV18] Andreas Loukas and Pierre Vandergheynst. „Spectrally Approximating Large Graphs with Smaller Graphs“. In: *Proceedings of the 35th International Conference on Machine Learning*. Ed. by Jennifer Dy and Andreas Krause. Vol. 80. Proceedings of Machine Learning Research. Stockholm, Sweden: PMLR, 2018, pp. 3237–3246. arXiv: 1802.07510v1 [cs.LG] (cit. on p. 24).
- [MH16] Vitalik Melnikov and Eyke Hüllermeier. „Learning to Aggregate Using Uninorms“. In: *Machine Learning and Knowledge Discovery in Databases*. Springer International Publishing, 2016, pp. 756–771 (cit. on pp. 3, 4).
- [MH19] Vitalik Melnikov and Eyke Hüllermeier. „Learning to Aggregate: Tackling the Aggregation/Disaggregation Problem for OWA“. In: *Proceedings of The Eleventh Asian Conference on Machine Learning*. Ed. by Wee Sun Lee and Taiji Suzuki. Vol. 101. Proceedings of Machine Learning Research. Nagoya, Japan: PMLR, 2019, pp. 1110–1125 (cit. on p. 5).
- [Mik+13] Tomas Mikolov, Ilya Sutskever, Kai Chen, Greg Corrado, and Jeffrey Dean. „Distributed Representations of Words and Phrases and Their Compositionality“. In: *Proceedings of the 26th International Conference on Neural Information Processing Systems - Volume 2*. NIPS’13. Lake Tahoe, Nevada: Curran Associates Inc., 2013, pp. 3111–3119. arXiv: 1310.4546v1 [cs.CL] (cit. on p. 17).
- [Mil02] R. Milo. „Network Motifs: Simple Building Blocks of Complex Networks“. In: *Science* 298.5594 (2002), pp. 824–827 (cit. on p. 12).
- [Mor+17] Christopher Morris, Kristian Kersting, and Petra Mutzel. „Glocalized Weisfeiler-Lehman Graph Kernels: Global-Local Feature Maps of Graphs“. In: *2017 IEEE International Conference on Data Mining (ICDM)*. IEEE, 2017. arXiv: 1703.02379v3 [cs.LG] (cit. on p. 20).
- [Mor+19] Christopher Morris, Martin Ritzert, Matthias Fey, et al. „Weisfeiler and Leman Go Neural: Higher-Order Graph Neural Networks“. In: *Proceedings of the AAAI Conference on Artificial Intelligence* 33 (2019), pp. 4602–4609. arXiv: 1810.02244v3 [cs.LG] (cit. on p. 24).

- [MP13] Brendan D. McKay and Adolfo Piperno. *Practical graph isomorphism, II*. Jan. 8, 2013. arXiv: 1301.1493v1 [cs.DM] (cit. on p. 7).
- [MW97] A. D. McNaught and A. Wilkinson. „functional group“. In: *IUPAC Compendium of Chemical Terminology*. 2nd ed. IUPAC, 1997, p. 1116 (cit. on p. 28).
- [Nar+17] Annamalai Narayanan, Mahinthan Chandramohan, Rajasekar Venkatesan, et al. *graph2vec: Learning Distributed Representations of Graphs*. July 17, 2017. arXiv: 1707.05005v1 [cs.AI] (cit. on p. 18).
- [New03] M. E. J. Newman. „The Structure and Function of Complex Networks“. In: *SIAM Review* 45.2 (2003), pp. 167–256 (cit. on p. 12).
- [Per+14] Bryan Perozzi, Rami Al-Rfou, and Steven Skiena. „DeepWalk: online learning of social representations“. In: *Proceedings of the 20th ACM SIGKDD international conference on Knowledge discovery and data mining - KDD '14*. ACM Press, 2014. arXiv: 1403.6652v2 [cs.SI] (cit. on p. 17).
- [She+11] Nino Shervashidze, Pascal Schweitzer, Erik Jan Van Leeuwen, Kurt Mehlhorn, and Karsten M. Borgwardt. *Weisfeiler-Lehman Graph Kernels*. 2011 (cit. on pp. 18, 19).
- [Shu+13] D. I. Shuman, S. K. Narang, P. Frossard, A. Ortega, and P. Vandergheynst. „The emerging field of signal processing on graphs: Extending high-dimensional data analysis to networks and other irregular domains“. In: *IEEE Signal Processing Magazine* 30.3 (2013), pp. 83–98 (cit. on pp. 13, 15).
- [Wel+07] Howard T. Welser, Eric Gleave, Danyel Fisher, and Marc Smith. „Visualizing the signatures of social roles in online discussion groups“. In: *Journal of Social Structure* (2007) (cit. on p. 12).
- [WL68] Boris Weisfeiler and Andrei A. Lehman. „A reduction of a graph to a canonical form and an algebra arising during this reduction“. In: *Nauchno-Technicheskaya Informatsia* 2.9 (1968), pp. 12–16 (cit. on p. 7).
- [Wu+19] Zonghan Wu, Shirui Pan, Fengwen Chen, et al. *A Comprehensive Survey on Graph Neural Networks*. Jan. 3, 2019. arXiv: 1901.00596v4 [cs.LG] (cit. on p. 21).
- [WW86] Peter Willett and Vivienne Winterman. „A Comparison of Some Measures for the Determination of Inter-Molecular Structural Similarity Measures of Inter-Molecular Structural Similarity“. In: *Quantitative Structure-Activity Relationships* 5.1 (1986), pp. 18–25 (cit. on p. 16).
- [Xu+19] Keyulu Xu, Weihua Hu, Jure Leskovec, and Stefanie Jegelka. „How Powerful are Graph Neural Networks?“ In: *International Conference on Learning Representations*. ICLR'2019. 2019. arXiv: 1810.00826v3 [cs.LG] (cit. on pp. 23, 24, 36).
- [Zha+18] Muhan Zhang, Zhicheng Cui, Marion Neumann, and Yixin Chen. „An end-to-end deep learning architecture for graph classification“. In: *Thirty-Second AAAI Conference on Artificial Intelligence*. 2018 (cit. on p. 25).
- [Gil+18] L. H. Gilpin, D. Bau, B. Z. Yuan, et al. „Explaining Explanations: An Overview of Interpretability of Machine Learning“. In: *2018 IEEE 5th International Conference on Data Science and Advanced Analytics (DSAA)*. 2018, pp. 80–89. arXiv: 1806.00069v3 [cs.AI] (cit. on p. 30).

Websites

- [Ban+18a] Priyanka Banerjee, Robert Preissner, Andreas Eckert, and Anna K. Schrey. *ProTox-II - Prediction Of Toxicity Of Chemicals*. Charité – Universitätsmedizin Berlin. 2018. URL: http://tox.charite.de/protox_II/ (visited on Nov. 18, 2019) (cit. on p. 16).
- [MP] Brendan McKay and Adolfo Piperno. *nauty and Traces*. URL: <http://pallini.di.uniroma1.it/index.html> (visited on Feb. 21, 2020) (cit. on p. 7).
- [Tes] *Toxicity Estimation Software Tool (TEST)*. EPA. URL: <https://www.epa.gov/chemical-research/toxicity-estimation-software-tool-test> (visited on Nov. 18, 2019) (cit. on p. 16).
- [Tox] *ToxTrack - Cheminformatics Modeling*. ToxTrack Inc. URL: <https://toxtrack.com/> (visited on Nov. 18, 2019) (cit. on p. 16).

List of Figures

| | | |
|------|--|----|
| 2.1 | Overview of the structure of LTA for multiset compositions. | 4 |
| 2.2 | The Łukasiewicz norms and the corresponding uninorm for $\lambda = 0.5$ | 5 |
| 2.3 | Illustration of how a BUM function is described as a linear spline and its relation to the OWA weights. | 6 |
| 2.4 | Example 1-WL color refinement steps. | 9 |
| 2.5 | Two simple non-isomorphic graphs that are indistinguishable by 1-WL. | 9 |
| 2.6 | WL neighborhoods for different values of k | 10 |
| 2.7 | Two non-isomorphic graphs with $G \simeq_1 H$ and $G \not\simeq_2 H$ | 11 |
| 2.8 | Comparison between the basis vectors of the real domain Fourier transform and the graph Fourier transform. | 15 |
| 2.9 | Comparison of the unnormalized L_G spectrum and the normalized L_G^{sym} spectrum. | 15 |
| 2.10 | Illustration of the correspondence between the WL color $\chi_{G,1}^{(t)}(v)$ and the breadth-first subtree of depth l rooted at v | 19 |
| 3.1 | Overview of the generalized LTA architecture for structured data. | 29 |
| 3.2 | The constituents implied by the WL subtree kernel embedding for an example graph. | 33 |
| 3.3 | An LTA perspective on GCNNs that use vertex neighborhood convolutions. . | 36 |

Erklärung zur Masterarbeit

Ich, Clemens Damke (Matrikel-Nr. 7011488), versichere, dass ich die Masterarbeit mit dem Thema *Learning to Aggregate on Structured Data* selbstständig verfasst und keine anderen als die angegebenen Quellen und Hilfsmittel benutzt habe. Die Stellen der Arbeit, die ich anderen Werken dem Wortlaut oder dem Sinn nach entnommen habe, wurden in jedem Fall unter Angabe der Quellen der Entlehnung kenntlich gemacht. Das Gleiche gilt auch für Tabellen, Skizzen, Zeichnungen, bildliche Darstellungen usw. Die Masterarbeit habe ich nicht, auch nicht auszugsweise, für eine andere abgeschlossene Prüfung angefertigt. Auf § 63 Abs. 5 HZG wird hingewiesen.

Paderborn, 20. März 2020

Clemens Damke